Juillet 1977
FR7800268

HIGH-SPIN STATES IN $^{104,\ 105}$Cd.

J. Genevey-Rivier, J. Tréherne,
Institut des Sciences Nucléaires, BP 257, Centre de Tri,
38044, Grenoble, Cedex (France)

and

J. Danière, R. Béraud, M. Meyer, R. Rougny,
Institut de Physique Nucléaire, (and IN2P3), Université Claude-Bernard
Lyon-I, 43 Bd du 11 Novembre 1918, 69621 Villeurbanne (France).

1 - INTRODUCTION

A considerable amount of experimental work has been done in the Cadmium nuclei, however very scarce information was available on the neutron-deficient ^{104}Cd and ^{105}Cd isotopes. The level structure of ^{105}Cd had been investigated in our group from the ^{105}In → Cd decay (Rougny et al. 1973, River et al. 1975). Recently in the single neutron pick-up reaction ^{106}Cd(^{3}He, α)^{105}Cd performed by Chapman and Dracoulis (1975), eleven states of the final nucleus were identified and corresponding ℓ_n - value assignments extracted.

A striking feature of ^{107}Cd (Hagemann et al. 1974) and ^{109}Cd (Meyer et al. 1975) nuclei is the existence of a decoupled band built on the unique parity ν(h 11/2) state. This led us to search for a similar sequence of high spin states connected by stretched E2 transitions in ^{105}Cd using Pd(α, xnγ)Cd reaction.

The study of ^{104}Cd was all the more important as in ^{106}Cd we observed (Danière et al. 1977) additional 6^+ and 8^+ levels probably due to particle excitation. In the case of ^{104}Cd nucleus only the two first excited levels were known from Mo(^{12}C, xnγ)^{104}Cd reaction (Hashizume et al.

1969). R. Coussement et al. (1976) observed 3 γ-rays in the (1.7 ± 0.3) min. ^{104}In decay using on-line mass separation techniques. Recently Varley et al. (1977) proposed a more detailed level scheme studying the same decay. The aim of the present work is to identify the high spin states of ^{104}Cd by ^{102}Pd(α, 2nγ)^{104}Cd reaction.

2 - EXPERIMENTAL PROCEDURE AND DATA ANALYSIS

Targets approximately 10 mg/cm^2 of isotopically enriched ^{104}Pd (80%) and ^{102}Pd (78%) were prepared by deposition on thin polyethylene backings. They were bombarded with 1 - 5 nA beams of α particles from the Grenoble variable energy cyclotron.

The γ-ray single spectra measurements were performed with a 40 cm^3 Ge(Li) detector at 45^{o} to the beam direction. The energy resolution of this calibrated spectrometer was 2.2 keV (F.W.H.M) for 1332.5 keV γ-rays of ^{60}Co.

γ-ray spectra were recorded at α bombarding energies ranging from 20 to 53 MeV in order to find the maximum γ-ray yield for ^{104}Cd and ^{105}Cd. These excitation functions led us to fix the energy at 33 MeV for the ^{102}Pd(α, 2n)^{104}Cd reaction. The ^{105}Cd nucleus was studied by two different reactions : ^{102}Pd(α, n)^{105}Cd at 24 MeV and ^{104}Pd(α, 3n)^{105}Cd at 43 MeV. Typical excitation function curves of the strongest lines in ^{105}Cd are presented in Figure 1 for the ^{104}Pd(α, 3n)^{105}Cd.

γ-γ coincidences were studied in separate experiments using two Ge(Li) detectors and a fast-slow coincidence circuit with overall time resolution about 10 ns. The coincidences were stored event by event on a magnetic tape connected to a PDP-9 computer. The data matrix was 1024 x 1024 channels and more than 2.10^7 events were stored for each isotope studied. An off-line analysis allowed the reconstruction of coincidence spectra by setting digital gates on the peaks of interest.

The γ-γ results were used in connection with the sum rule for the construction of the level scheme.

Additionnal HF-γ delayed coincidence measurements were performed in order to search for long-lived levels. For this, γ-ray spectra delayed and not delayed with respect to the high frequency signal, called respectively "OUT" and "IN" spectra have been recorded.

The angular distribution experiments were performed with the targets mentioned above. For the $^{102}Pd(\alpha, n)^{105}Cd$ reaction, the maximum recoil energy is ≈ 1.3 MeV with bombarding α particles of 33 MeV energy. Then the corresponding range of the Cd nuclei is about 0.3 mg/cm^2 in a $A = 102$ matrix (Northcliffe and Shilling, 1970). Thus at least 98% of the recoiling nuclei are stopped in our target ; this is corroborated by the fact that the angular distribution spectra do not exhibit any distortion due to Doppler shift.

Beam centering was checked by measuring the angular distribution γ-rays due to the $^{105}Cd \rightarrow Ag$ radioactivity produced in the target (accuracy better than 0.5%). A third detector located at a fixed position ($+ 60^{o}$) was used for beam intensity monitoring. The overall error on the normalization was about 1% for both nuclei.

The target-to-detector distance was 13.5 cm and the detector was positioned at 5 angles from $- 90^{o}$ to $- 150^{o}$ with respect to the beam axis. Two complete cycles were made with 30 minutes counting period at each angle. The angular distributions have been analyzed in a classical way, described earlier by Yamazaki (1967) and Simms et al. (1973) for example, assuming that the nucleus was excited into an approximately aligned state with a Gaussian population of magnetic sub-states centered on $m = 0$. We have checked the consistency of our measurement by extracting the σ/I values from the attenuation of the A_2 and A_4 coefficients.

3 - RESULTS FOR ^{104}Cd

On figure 2 is plotted a direct γ-ray spectrum obtained in the ^{102}Pd(α, 2nγ)^{104}Cd reaction at 33 MeV energy projectile. As an example of γ-γ coincidences, figure 3, shows typical coincidence spectra gated by the 532.9, 840.6 and 890.2 keV γ lines. In these spectra appear the 657.9 ($2^+ \rightarrow 0^+$) and 834.0 keV ($4^+ \rightarrow 2^+$) γ rays unambigously assigned to ^{104}Cd isotope by Varley et al. (1977). Table I summarizes the properties of γ-rays assigned to this isotope. On figure 4 are plotted the least square fits of angular distribution for the transitions appearing in the strongest cascade of ^{104}Cd. From HF-γ delayed coincidence measurements there is no evidence of a long-lived state in this nucleus ; we now discuss relevant points of our scheme presented in figure 5.

657.9 and 1491.9 keV levels

Angular distributions ($\Delta I = 0, -2$) of 657.9 and 834.0 keV γ-rays and the absence of "cross-over" 1491.9 keV transition allow to confirm the assignment 2^+ and 4^+ for these levels, recently made by Varley et al. (1977) and previously by Hashizume et al. (1969).

2114.0 keV level

This level could be the level observed at 2116 keV excitation energy by Varley et al. (1977) in the ^{104}In decay. The $\Delta I = 0, -2$ character of the 321.2 keV γ-line connecting the 6^+ level at 2435.4 keV (as shown above) and the 622 keV γ-ray allow to propose 4^+.

2370.0, 3210.7 and 4100.9 keV levels

The angular distribution of the 878.1 keV, 840.6 keV and 890.2 keV γ-rays are typicaly stretched E2 transitions. The non-existence of "cross-over" transitions ($I \rightarrow I - 4$) leads us to assign the 6^+, 8^+, 10^+ spins sequence.

2435.4 , 2843.7 and 2902.0 keV levels

The E2 character of the 775.3 keV clearly indicates the spin 6^+ for the 2435.4 keV level. From the angular distribution results of the 473.7 and 532.9 keV transitions ($\Delta I = 0, -2$) we assign spin 6 or 8 for both levels 2843.7 and 2902.0 keV.

3903.9 , 4038.3 and 4741 keV levels

The $\Delta I = \pm 1$ character of both 1001.0 keV and 827.6 keV transitions gives 5, 7 or 9 as possible spin for the 3903.9 keV level and 7, 9 for the 4038.3 keV level. Taking into account the angular distribution of the 702 keV γ-line, we assign the spin 9, 11 to the 4741 keV level.

4 - RESULTS FOR ^{105}Cd

Table II gives a summary of the data obtained about the γ-rays assigned to ^{105}Cd in the ^{102}Pd(α, n)^{105}Cd reaction. On figure 6 a single γ spectrum is presented. The γ-ray intensity ratios reported in table III show that the 126.4 keV - 812.5 keV - 807.8 keV cascade is delayed and partially fed by an isomeric level. This is in agreement with the identification by Heiser et al. (1973) of a 5 μs halflife level at an excitation energy higher than 2517.2 keV. This was confirmed later by Grau et al. (1975). Figure 7 represents two coincidence spectra gated by the 539.3 and 668 keV γ-rays. Let us now discuss in more details the most interesting features of the level scheme shown in figure 8.

g.s. 195.9 and 260.0 keV levels

Spin and parity $5/2^+$ of the g. s. level were assigned by Laulainen and Mc. Dermott (1969) from hyperfine structure studies using the optical double-resonance technique and confirmed in ^{106}Cd(d, t)^{105}Cd reaction (Degnan and Rao, 1973) and more recently by Chapman and Dracoulis (1975) in ^{106}Cd(^{3}He, α)^{105}Cd reaction. The 195.9 keV level has been already observed by Rougny et al. (1973) in the 5.1 min ^{105}In decay. The angular distribution of the (195 keV → g.s.) transition could not be evaluated because of the presence of the 197 γ-line due to ^{19}F activity produced by $^{16}O(\alpha, p)^{19}F$ reaction. Probable spin values are ranging from 1/2 to 9/2.

1162.7, 1702.0, 2488.2, 3343.9 keV levels

The angular distributions of the 539.3, 786.2 and 854.7 keV γ-rays are characteristic of stretched E2 transitions. So we assign the spin sequence $11/2^-$, $15/2^-$, $19/2^-$, $23/2^-$. It must be noted that the negative parity of the 11/2 (1162.7 keV) state has been recently proposed by Grau et al. (1975).

131.1, 799.2, 1685.8, 2587.3 keV levels

For the 131.1 keV level, the result of the angular distribution of the 131 keV γ-ray ($\Delta I = \pm 1$) is in agreement with the reaction data giving $\ell_n = 4$ with $7/2^+$ assignment. The angular distributions of the 668.1, 886.6 and 901.5 keV γ-rays are characteristic of stretched E2 transitions : so we assign $11/2^+$, $15/2^+$, $19/2^+$ for the 799.2, 1685.8 and 2587.3 keV levels.

604.1, 770.5, 1578.4, 2390.8 keV levels

From the angular distributions of the 604.1 keV ($\Delta I = \pm 1$), 770.5 keV, 807.8 keV, 812.5 keV ($\Delta I = -2$) γ-rays we propose $7/2^+$, $9/2^+$, $13/2^+$ and $17/2^+$ respectively for these states.

832.2, 1728.2 keV levels

The angular distributions of the 832.2, 227.8 and 700.9 keV γ-rays allow to assign unambigously $I^\pi = 9/2^+$ for the 832.2 keV level. The large A_2 coefficient of the 896 keV angular distribution favours $\Delta I = -2$ and led us to propose $13/2^+$ for the 1728.2 keV level.

5 - DISCUSSION

^{104}Cd

We discuss the structure of the ^{104}Cd nucleus (see figure 9) in connection to that of ^{106}Cd and heavier isotopes (Cochavi et al. (1971) for ^{108}Cd and Lumpkin et al. (1974) for ^{110}Cd). Hartree-Fock calculations have been performed using the Skyrme interaction and the potential energy curves versus the deformation exhibits a wide minimum subdivised into two minima for $^{102-106-110}$Cd isotopes (Meyer et al. (1976). This confirms that e. e. Cd nuclei are very soft transitional nuclei, with a weak but clear prolate deformation. For positive parity states, up to the 6^+ state, the ground state band is similarly developped in $^{104-106-108-110}$Cd. But another 6^+ state with similar feeding and located at the same energy appears both in $^{104-106}$Cd, in contrast with the $^{108-110}$Cd nucleus. In this even-even nuclei, we should observe at least by (α, xnγ) reaction, the band-head of decoupled bands built on two-quasi particles states ($I = j_1 + j_2 + R$) such as the aligned pairs ($\nu d5/2\ \nu g7/2$) 6^+ or higher in energy $(\nu h11/2)^2 10^+$, $(\pi g9/2)^{-2} 8^+$. Similar bands have been recently observed in even Pd nuclei (Grau et al. (1976)). In the heavier isotopes $^{108-110}$Cd this phenomena would only occurs from 8^+ and 10^+ because the fermi level goes upper ($N = 62-60$) and the d5/2 and g7/2 orbitals are nearly filled. A similar explanation of this situation is given by the Arima and Iachello model (Arima and Iachello (1976) which takes into account the number of bosons (or pairs of neutrons) outside the $N = 50$ closed shells : $^{104}_{48}Cd_{56}$ $N = 3$, $^{106}Cd_{58}$ $N = 4$, $^{108}Cd_{60}$ $N = 5$, $^{110}Cd_{62}$ $N = 6$ and predicts a "cut-off" of the ground state band from respectively the 6^+, 8^+, 10^+ and 12^+.

For the negative parity states we have some candidates to be the $(\nu h11/2, \nu g7/2)_{9^-}$ or $(\nu h11/2\ \nu d5/2)_{8^-}$ band head states but they are located higher in energy than in $^{108-110}$Cd because of the ascending behaviour of the $\nu h11/2$ neutron orbital.

^{105}Cd

The most stricking feature of our results is the existence of a $\Delta I = 2$ negative band which exhibits a spin sequence $11/2^-$, $15/2^-$, $19/2^-$, ($23/2^-$). The energy spacing appears quite comparable to that of 0^+, 2^+, 4^+, 6^+ states of the even ^{104}Cd core. So we refer to these $11/2^-$, $15/2^-$, $19/2^-$, ($23/2^-$) states as rotation aligned states where the angular momentum of the odd-particle (here the 1h11/2 unique parity neutron orbital) is aligned to that of the core R giving states $I = j + R = j$, $j + 2$, $j + 4$ etc.. Similar negative parity "decoupled" bands have already been observed by (α, xnγ) reactions, in $^{107-109}$Cd nuclei (see figure 10). In the charac ter of the $11/2^-$ $\Delta I = 2$ decoupled band remains unchanged the feeding of this band is less in ^{105}Cd than in $^{107-109}$Cd : when A decreases, the 1h11/2 neutron orbital lies at a higher energy. We can note that the so-called "anti-aligned" states $I = | j - R |$ have not been observed in these (α, xnγ) reactions.

For the positive parity states, one could expect a similar decoupling for the highest - j positive parity orbitals, namely 1g7/2 and even 2d5/2 as observed in $^{101-103-105}$Pd (Rickey and Simms (1973)). The $\Delta I = 2$ band built on the 1g7/2 neutron orbital ($7/2^+$, $11/2^+$, $15/2^+$) has been tentatively observed in ^{109}Cd and ^{107}Cd, but in ^{105}Cd this decoupled band is definitly present and strongly fed (see figure 10).

Concerning the band based on the 2d5/2 orbital, which is rather strongly fed in ^{105}Cd as compared to the heavier isotopes, its caracter is not clearly defined. This band seems to be perturbed by Coriolis effects because $\Delta I = 1$ and $\Delta I = 2$ transitions both occur. Its decoupled character will probably strengthen when N decreases as in ^{105}Pd, ^{103}Pd, ^{101}Pd and it would be worth to follow the evolution of such $5/2^+$ bands in lighter isotopes. In figure 11, are presented the lowest levels of a given spin for the $^{109-107-105}$Cd ; one can observe a compression of the whole spectrum when N decreases.

In conclusion, we have seen in ^{104}Cd isotope that from the 6^+ level of the ground-state band, several particle states appear and that rotation-aligned bands would intersect. For these even-even nuclei, calculations including both neutron and proton excitations in a Coriolis treatment would be of high interest.

We have shown that ^{105}Cd isotope exhibits two interesting features :

- decoupled bands built on $\nu h11/2$ and $\nu g7/2$ orbitals

- a strongly perturbed band built on $\nu d5/2$ that should become decoupled in $^{103-101}Cd$ nuclei. The knowledge of the B(E2) transition values would be a crucial test for these positive parity bands.

Acknowlegments

We are very indebted to the Grenoble Cyclotron staff for cooperation during this work. The authors would like to thank Dr. Ph. Quentin and Dr. F. Iachello for valuable discussions.

REFERENCES

- Arima A., and Iachello F., 1976, Annals of Physics, 99, 253

- Chapman R., and Dracoulis G. D., 1975, J. Phys. G : Nucl. Phys., 1, 657

- Cochavi S., Mateosian E., Der Kistner O.C., Sunyar A.W., and Thieberger P., 1971, Bull. Amer. Phys. Soc., 16, 642

- Coussement R., De Raedt J., Dumont G., Huyse M., Lhersonneau G., Pacholski S., Pattyn H., Sastry D. L., and Van Klinken J., 1976 Proc. 3rd Int. Conf. on Nuclei far from Stability, CERN 76-13, p. 51

- Danière J., Béraud R., Meyer M., Rougny R., Genevey-Rivier J. and Treherne J., 1977, Z. Phys., A 280, 363

- Degnan J.H., and Rao C.R., 1973, Phys. Rev., C 7, 2131

- Grau J.A., Samuelson L.E., Popik S.I., Rickey F.A., and Simms P.C., 1975, Bull. Amer. Phys. Soc., 20, 721

- Grau J.A., Samuelson L.E., Rickey F.A., Simms P.C., and Smith G.J., 1976, Phys. Rev., C 14, 2297

- Hagemann U., Brickmann H.F., Fromm W.D., Heiser C., and Rotter H., 1974, Nucl. Phys., A 228, 112

- Hashizume A., Inamura T., Katou T., Tendow Y., Yamazaki T., and Nomura T., 1969, IPCR Cyclotron Progress Report, 3, 57

- Heiser C., Brinchmann H.F., Fromm W.D., Hagemann U., and Rotter H., 1973, Symposium on Nuclear Spectroscopy and Nuclear Theory, Dubna, June 19-23, 81

- Laulainen N.S., and Mc Dermott M.N., 1969, Phys. Rev., 177, 1615

- Lumpkin A. H., Sunyar A. W., Hardy K. A., and Lee Y. K., 1974, Phys. Rev., C 9, 258

- Meyer M., Béraud R., Danière J., and Rougny R., 1975, Phys. Rev., C 12, 1858

- Meyer M., Danière J., Letessier J., and Quentin P., 1976 European Conference on Nuclear Physics with Heavy Ions, Caen, September 6-10, 98

- Northcliffe L. C., and Shilling R. F., 1970, Nucl. Data Tables, 7

- Rickey F. A., and Simms P. C., 1973, Phys. Rev. Lett., 31, 404

- Rivier J., and Moret R., 1975, Radiochemica Acta, 22, 27

- Rougny R., Meyer-Lévy M., Béraud R., Rivier J., and Moret R., 1973, Phys. Rev., C-8, 2332

- Simms P. C., Anderson R., Rickey F. A., Smith G., Steffen R. M., and Tesmer Jr., 1973, Phys. Rev., C 7, 1631

- Varley B. J., Cunnane J. C., and Gelletly W., 1977, J. Phys. G : Nucl. Phys., 3, 55

- Yamazaki T., 1967, Nucl. Data Tables, A-3

FIGURE CAPTIONS

Figure 1 : Relative yield versus energy for the strongest γ-rays observed in the reaction $^{104}Pd(\alpha, 3n)^{105}Cd$.

Figure 2 : Direct γ-ray spectrum obtained in the $^{102}Pd(\alpha, 2n\gamma)^{104}Cd$ reaction at 33 MeV energy projectile.

Figure 3 : Coincident γ-ray spectra gated by :
a) the 532.9
b) 840.6
c) 890.2 keV γ-rays.

Figure 4 : Least-square fits of angular distributions for the strongest γ-rays of ^{104}Cd.

Figure 5 : Level scheme of ^{104}Cd nucleus deduced from our experiments.

Figure 6 : Direct γ-ray spectrum obtained in the $^{102}Pd(\alpha, n)^{105}Cd$ reactions at 24 MeV energy projectile.

Figure 7 : Coincident γ-ray spectra gated by
a) 539.3
b) 668 keV γ-rays.

Figure 8 : Level scheme of ^{105}Cd nucleus deduced from our experiments.

Figure 9 : Systematics of excited states of $^{104-106-108-110}Cd$ isotopes.

Figure 10 : Comparison between negative and positive parity bands in $^{105-107-109}Cd$ isotopes and the gound-states band in neighbouring e-e $^{104-106-108-110}Cd$ nuclei.

Figure 11 : Experimental trend of favoured levels in $^{105-107-109}Cd$ isotopes.

TABLE CAPTIONS

Table I : Summary of the γ-ray data for ^{104}Cd from $^{102}Pd(\alpha, 2n\gamma)$ reaction. γ lines noted with * are complex and can be placed twice in the scheme. (The energy and intensity of the 559 keV line has been obtained from the coincidence data).

Table II : Summary of the γ-ray data for ^{105}Cd from $^{102}Pd(\alpha, n)^{105}Cd$.

Table III : γ-intensity ratios of some transitions delayed ("OUT") or non delayed ("IN") with respect to the high frequency signal of the cyclotron.

Transition (keV)	126.4	812.5	807.8	770.5
γ-Intensity ratio $\left(\frac{OUT}{IN}\right)$	1	0.17	0.035	0.025

Table I

E_γ (keV)		I_γ (E_α = 33 MeV)		Angular distrib. coeff. E_α = 33 MeV A_2	Angular distrib. coeff. E_α = 33 MeV A_4	Assignment $E_i \rightarrow E_f$		Assignment ΔI
187.4	(0.2)	10	(5)	+ 0.25 ± 0.14	- 0.18 ± 0.20	3031.1 →	2843.7	0, - 2
307.2	(0.3)	25	(4)	- 0.07 ± 0.06	+ 0.22 ± 0.08	3210.7 →	2902.9	± 1
321.2	(0.2)	53	(7)	+ 0.23 ± 0.04	- 0.12 ± 0.05	2435.4 →	2114.0	0, - 2
414.2	(0.3)	~ 5				4741.4 →	4327.2	
423.3	(0.3)	17	(3)	- 0.15 ± 0.07	- 0.09 ± 0.09	4327.2 →	3903.9	
467.3	(0.3)	10	(4)	+ 0.27 ± 0.22	- 0.10 ± 0.30	2902.9 →	2435.4	
473.7	(0.2)	20	(5)	+ 0.13 ± 0.10	- 0.14 ± 0.13	2843.7 →	2370.0	0, - 2
499.6	(0.2)	54	(10)	- 0.36 ± 0.04	+ 0.04 ± 0.06	3031.1 →	2531.5	± 1
532.9	(0.2)	150	(20)	+ 0.28 ± 0.02	- 0.18 ± 0.03	2902.9 →	2370.0	0, - 2
559	(1)	~ 15				4463 →	3903.9	
622.1	(0.2)*	{ 60	(25)	+ 0.21 ± 0.02	- 0.06 ± 0.03	3653.2 →	3031.1	
		{ 50	(25)			2114.0 →	1491.9	
634.6	(0.2)	30	(15)			4735.5 →	4100.9	
657.9	(0.2)	1000		+ 0.25 ± 0.01	- 0.12 ± 0.02	657.9 →	0	0, - 2
702.6	(0.2)	42	(7)	+ 0.29 ± 0.04	- 0.13 ± 0.06	4741.4 →	4038.3	0, - 2
716.8	(0.2)	16	(5)			4817.7 →	4100.9	
740.6	(0.3)	15	(5)			4394.4 →	3653.2	
775.3	(0.2)	86	(13)	+ 0.34 ± 0.03	- 0.20 ± 0.05	3210.7 →	2435.4	0, - 2
827.6	(0.2)	45	(8)	- 0.21 ± 0.05	+ 0.11 ± 0.07	4038.3 →	3210.7	± 1
834.0	(0.2)	990	(150)	+ 0.27 ± 0.01	- 0.12 ± 0.02	1491.9 →	657.9	0, - 2
840.6	(0.2)	126	(19)	+ 0.31 ± 0.03	- 0.18 ± 0.05	3210.7 →	2370.0	0, - 2
856.4	(0.3)	10	(5)			3887.5 →	3031.1	
878.1	(0.2)	510	(80)	+ 0.29 ± 0.02	- 0.13 ± 0.03	2370.0 →	1491.9	0, - 2
890.2	(0.2)	113	(16)	+ 0.31 ± 0.03	- 0.14 ± 0.04	4100.9 →	3210.7	0, - 2
927.6	(0.3)	60	(9)	+ 0.09 ± 0.02	- 0.22 ± 0.03	3297.6 →	2370.0	0, - 2
943.5	(0.3)	143	(20)	+ 0.08 ± 0.01	- 0.23 ± 0.02	2435.4 →	1491.9	0, - 2
1001.0	(0.3)	85	(13)	- 0.11 ± 0.02	0 ± 0.03	3903.9 →	2902.9	± 1
1039.6	(0.3)	37	(6)	+ 0.23 ± 0.06	+ 0.05 ± 0.06	2531.5 →	1491.9	0, ± 1
1356.0	(0.3)	15	(5)			3887.5 →	2531.5	

Table II

E_γ (keV)		I_γ (E_α = 24 MeV)		Angul. distrib. coeff. A_2	A_4	Assignment $E_i \rightarrow E_f$	Δ_I
126.4	(0.2)	30	(2)	+ 0.02 ± 0.09	- 0.14 ± 0.16	2517.2 → 2390.8	
131.1	(0.2)	1000		- 0.176 ± 0.014	- 0.033 ± 0.016	131.1 → 0	± 1
166.4	(0.2)	36	(3)	- 0.20 ± 0.08	+ 0.11 ± 0.13	770.5 → 604.0	± 1
195.9	(0.2)	260	(14)			195.9 → 0	
227.8	(0.2)	42	(6)	- 0.31 ± 0.09	0 ± 0.14	832.0 → 604.0	± 1
260.0	(0.2)	500	(30)	+ 0.20 ± 0.02	+ 0.030 ± 0.026	260.0 → 0	0, ± 1
330.6	(0.2)	190	(20)	- 0.28 ± 0.03	- 0.01 ± 0.04	1162.7 → 832.0	± 1
392.0	(0.3)	210	(15)	- 0.27 ± 0.03	- 0.02 ± 0.04	1162.7 → 770.5	± 1
415.3	(0.3)	54	(7)				
472.8	(0.3)	35	(6)			604.0 → 131.1	
510.6	(0.3)	200	(100)			770.5 → 260.0	
539.3	(0.2)	330	(30)	+ 0.28 ± 0.03	- 0.13 ± 0.04	1702.0 → 1162.7	0, - 2
570.9	(0.3)	61	(6)	+ 0.17 ± 0.10	- 0.20 ± 0.17	766.8 → 195.9	0, - 2
604.1	(0.2)	300	(20)	- 0.73 ± 0.03	+ 0.10 ± 0.05	604.0 → 0	± 1
639.5	(0.2)	300	(50)	- 0.17 ± 0.03	+ 0.16 ± 0.04	770.5 → 131.1	± 1
668.1	(0.2)	910	(70)	+ 0.30 ± 0.02	- 0.12 ± 0.03	799.2 → 131.1	0, - 2
700.9	(0.2)	61	(6)	- 0.82 ± 0.10	- 0.13 ± 0.15	832.0 → 131.1	± 1
704.9	(0.3)	19	(10)	- 0.73 ± 0.30	+ 0.4 ± 0.4	2390 → 1685.8	± 1
770.5	(0.2)	125	(15)	+ 0.35 ± 0.05	- 0.13 ± 0.09	770.5 → 0	0, - 2
779.2	(0.3)	37	(10)	- 0.85 ± 0.15	+ 0.1 ± 0.2	1578.4 → 799.2	± 1
786.2	(0.2)	130	(20)	+ 0.29 ± 0.05	- 0.14 ± 0.08	2488.2 → 1702.0	0, - 2
807.8	(0.2)	260	(30)	+ 0.30 ± 0.04	- 0.12 ± 0.06	1578.4 → 770.5	0, - 2
812.5	(0.2)	65	(10)	+ 0.14 ± 0.11	- 0.13 ± 0.18	2390.8 → 1578.4	0, - 2
832.2	(0.2)	600	(60)	+ 0.30 ± 0.02	- 0.08 ± 0.04	832.0 → 0	0, - 2
854.7	(0.2)*	42	(5)	- 0.20 ± 0.17	- 0.16 ± 0.27	3342.9 → 2488.2 1115 → 260	
886.6	(0.3)	400	(40)	+ 0.29 ± 0.03	- 0.07 ± 0.04	1685.8 → 799.2	
896.0	(0.3)	150	(15)	+ 0.33 ± 0.07	+ 0.05 ± 0.10	1728.2 → 832.0	0, ±1, -2
901.5	(0.3)	70	(10)	+ 0.38 ± 0.10	- 0.29 ± 0.17	2587.3 → 1685.8	0, - 2
915.0	(0.4)	9	(5)			2643.2 → 1728.2	
943.6	(0.4)	20	(4)			1139.5 195.9	
1115.1	(0.4)	17	(5)			1115.1 → 0	
1125.7	(0.4)	11	(10)			1385.5 → 260.0	
1139.8	(0.4)	25	(20)			1139.5 → 0	
1189.3	(0.3)	50	(10)			1385.5 → 195.9	
1385.3	(0.4)	30	(15)			1385.5 → 0	

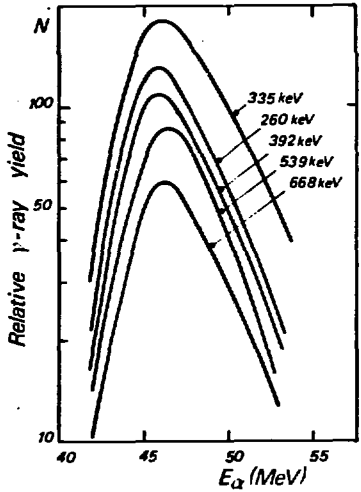

Relative γ-ray yield
N
100
50
10
40
45
50
55
Eα (MeV)
335 keV
260 keV
392 keV
539 keV
668 keV

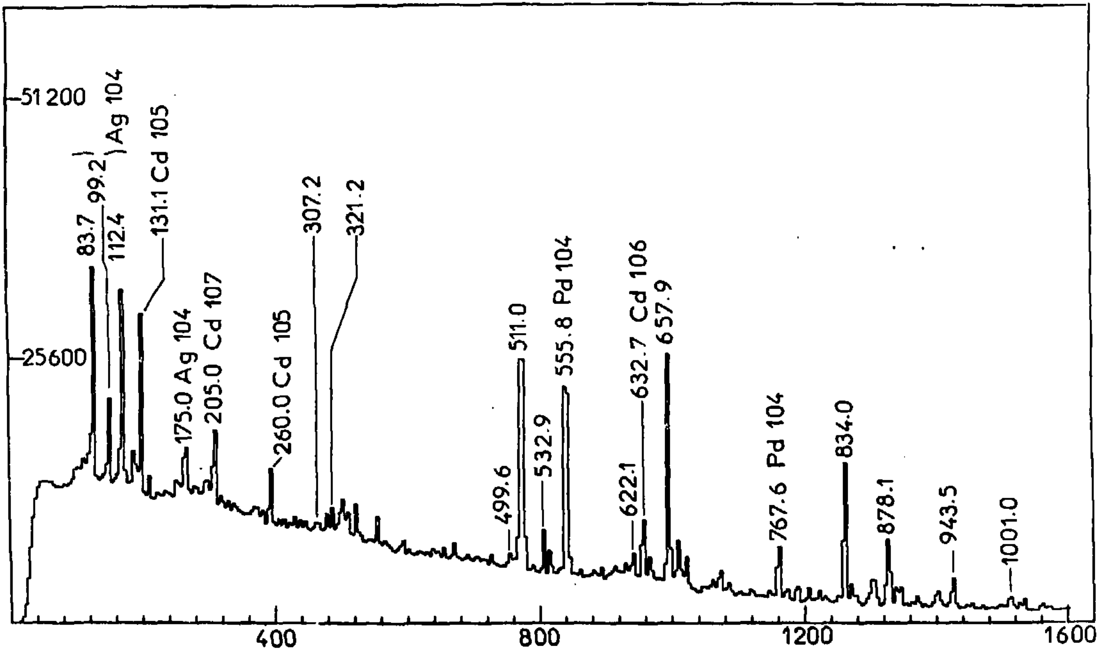

51200
25600
83.7
99.2
Ag 104
112.4
131.1 Cd 105
175.0 Ag 104
205.0 Cd 107
260.0 Cd 105
307.2
321.2
499.6
511.0
532.9
555.8 Pd 104
622.1
632.7 Cd 106
657.9
767.6 Pd 104
834.0
878.1
943.5
1001.0
400
800
1200
1600

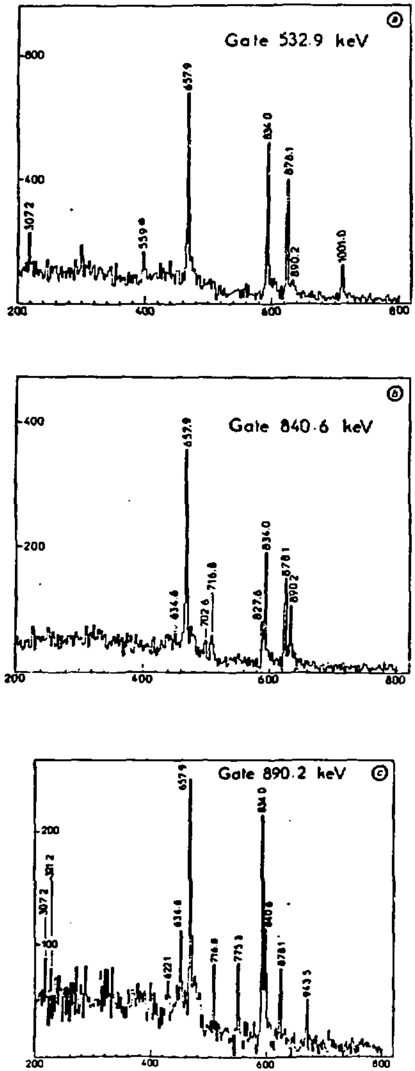

a
Gate 532.9 keV
600
400
200
800
307.2
559.
657.9
834.0
878.1
890.2
1001.0
b
Gate 840.6 keV
400
200
800
634.8
657.9
702.6
716.8
827.6
834.0
878.1
890.2
c
Gate 890.2 keV
100
800
307.2
634.8
657.9
716.8
834.0
840.6
878.1

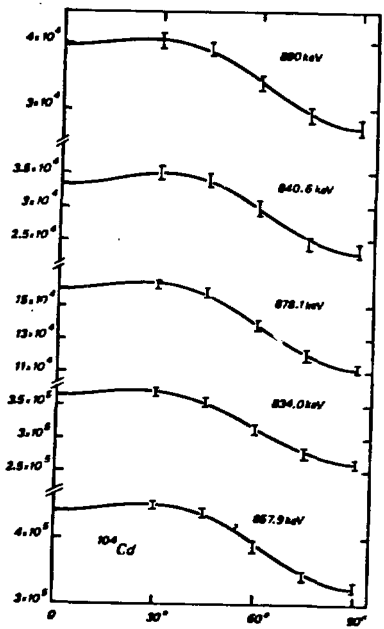

4.10⁴
3.10⁴
880 keV
3.5.10⁴
3.10⁴
2.5.10⁴
840.6 keV
15.10⁴
13.10⁴
11.10⁴
878.1 keV
3.5.10⁵
3.10⁵
2.5.10⁵
834.0 keV
4.10⁵
3.10⁵
867.9 keV
104Cd
0
30°
60°
90°

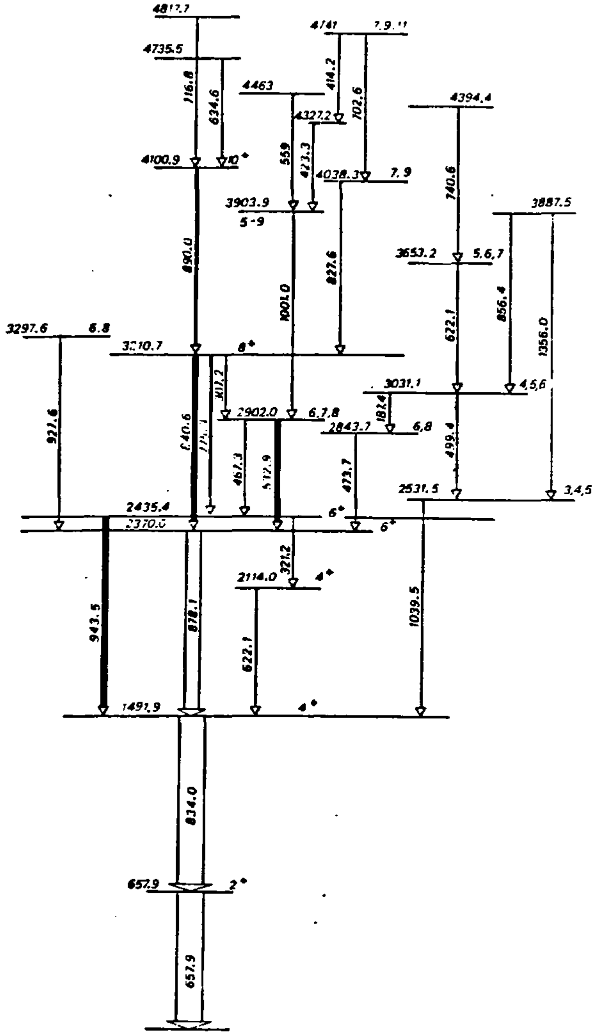
4817.7
4735.5
4741
7.9.11
4463
4327.2
4394.4
4100.9
10+
4038.3
7.9
3903.9
5-9
3887.5
3653.2
5,6,7
3297.6
6.8
8+
3031.1
4,5,6
2902.0
6.7.8
2843.7
6,8
2531.5
3,4,5
2435.4
6+
6+
2114.0
4+
1491.9
4+
657.9
2+
716.8
634.6
414.2
702.6
559
423.3
740.6
890.0
1001.0
827.6
622.1
856.4
1356.0
921.6
181.2
182.4
499.4
467.3
473.7
321.2
943.5
878.1
622.1
1039.5
834.0
657.9

^{104}Cd

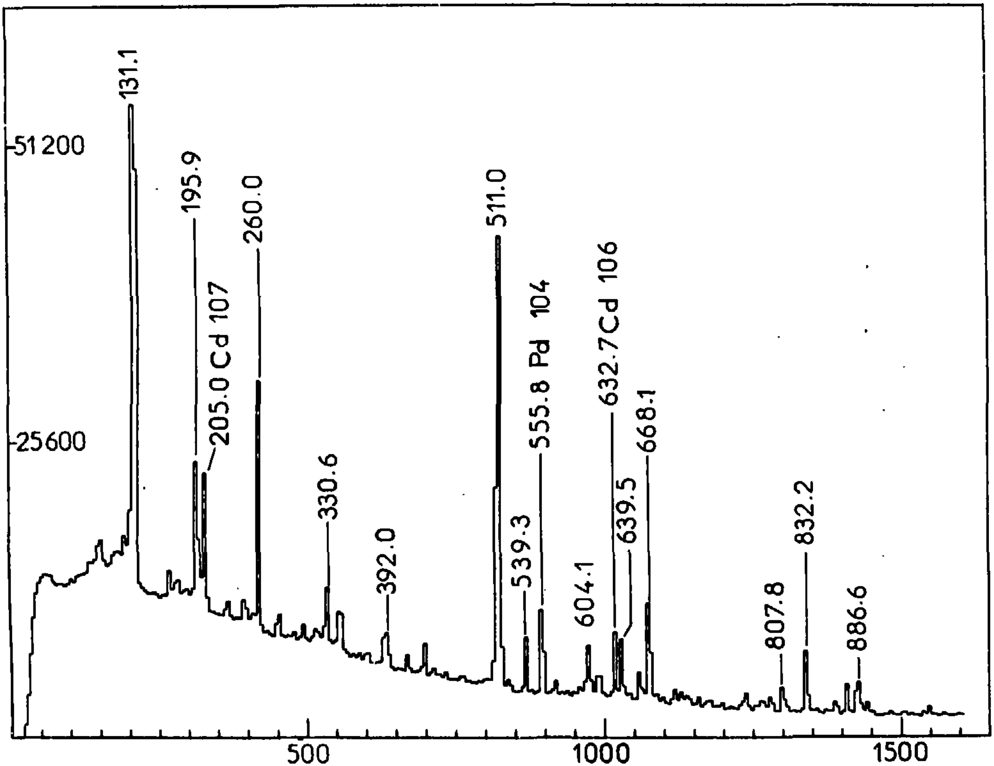

51200
25600
131.1
195.9
205.0 Cd 107
260.0
330.6
392.0
511.0
539.3
555.8 Pd 104
604.1
632.7Cd 106
639.5
668.1
807.8
832.2
886.6
500
1000
1500

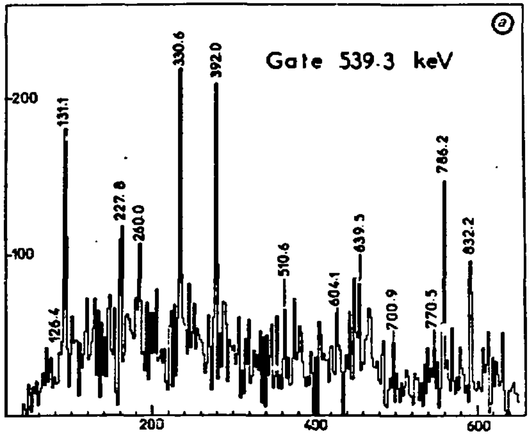
(a)
Gate 539.3 keV
200
100
131.1
126.4
227.8
260.0
330.6
392.0
510.6
604.1
639.5
700.9
770.5
786.2
832.2
200
400
600

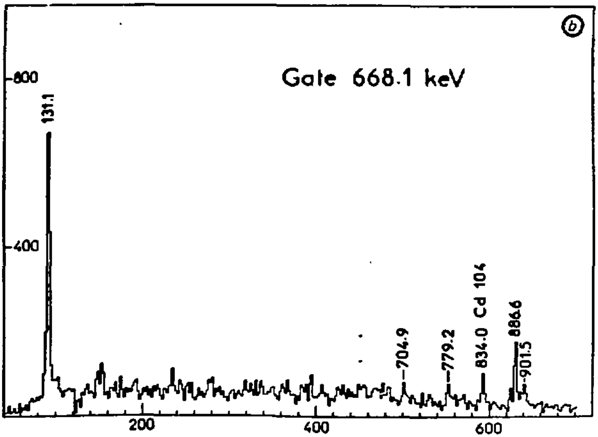
(b)
Gate 668.1 keV
800
400
131.1
704.9
779.2
834.0 Cd 104
886.6
901.5
200
400
600

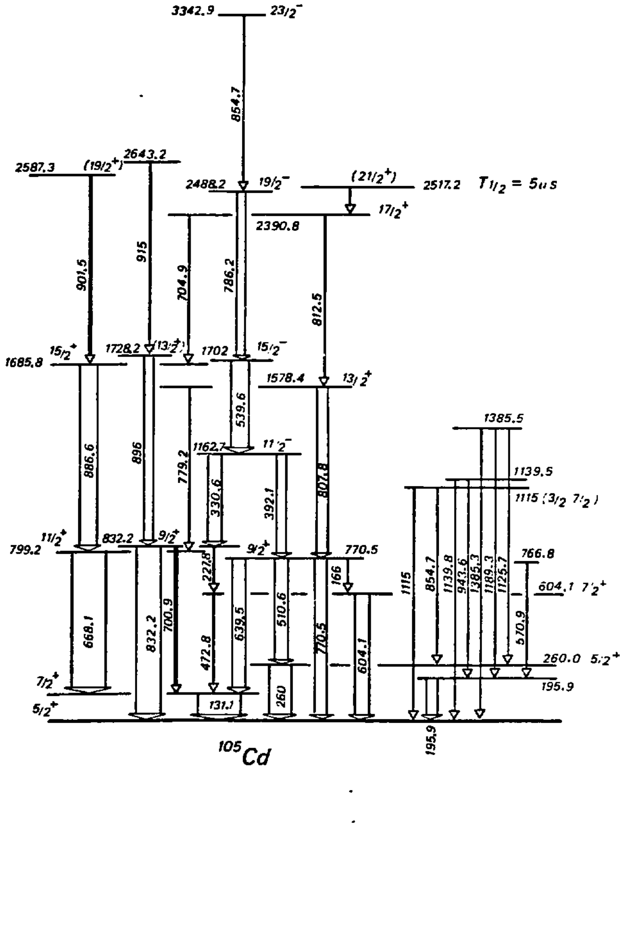
3342.9
23/2⁻
854.7
2587.3
(19/2⁺)
2643.2
2488.2
19/2⁻
(21/2⁺)
2517.2
T1/2 = 5us
17/2⁺
2390.8
901.5
915
704.9
786.2
812.5
1685.8
15/2⁺
1728.2
(13/2⁺)
1702
15/2⁻
1578.4
13/2⁺
539.6
886.6
896
779.2
1162.7
11/2⁻
330.6
392.1
807.8
1385.5
1139.5
1115 (3/2 7/2)
799.2
11/2⁺
832.2
9/2⁺
9/2⁺
770.5
166
766.8
604.1 7/2⁺
668.1
832.2
700.9
227.8
472.8
639.5
510.6
770.5
604.1
1115
854.7
1139.8
943.6
1385.3
1189.3
1125.7
570.9
260.0 5/2⁺
195.9
7/2⁺
5/2⁺
131.1
260
195.9
105Cd

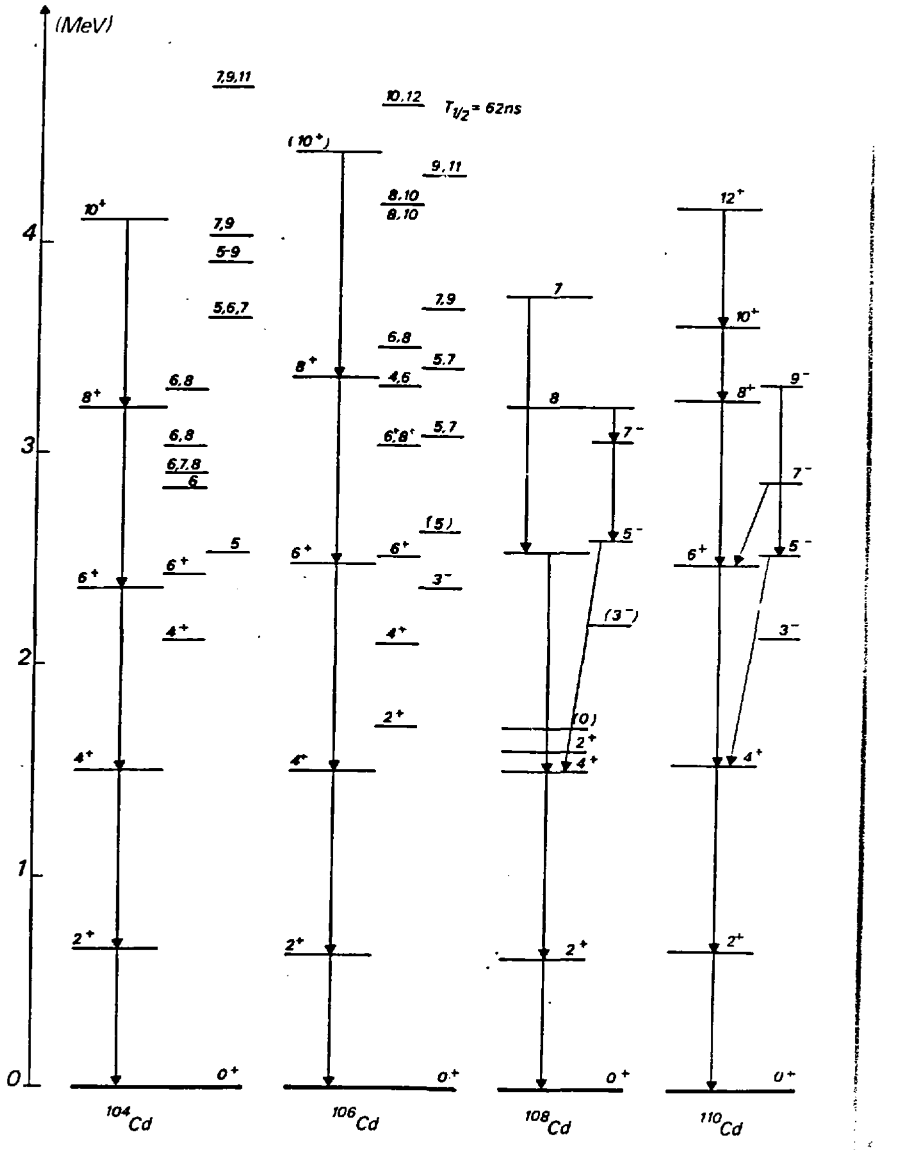
(MeV)
0
1
2
3
4
T1/2 = 62ns
104Cd
106Cd
108Cd
110Cd
0+
2+
4+
6+
8+
10+
(10+)
12+
7,9,11
10,12
9,11
8,10
8,10
7,9
5-9
5,6,7
6,8
6,7,8
6
5
4,6
5,7
6+8+
(5)
3-
(3-)
(0)
7
8
7-
5-
9-

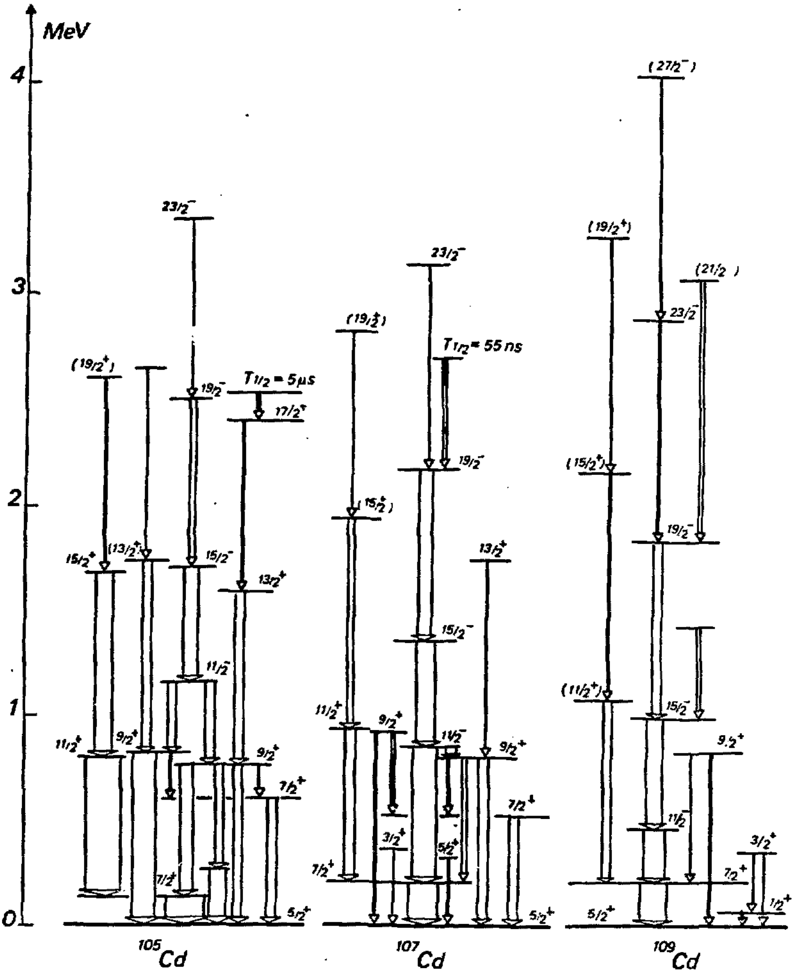

MeV
4
3
2
1
0
(27/2⁻)
23/2⁻
(19/2⁺)
(21/2)
$T_{1/2}$ = 5 μs
$T_{1/2}$ = 55 ns
105Cd
107Cd
109Cd

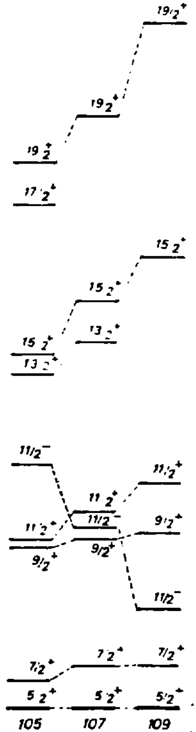

19/2+
19/2+
19/2+
17/2+
15/2+
15/2+
13/2+
15/2+
13/2+
11/2−
11/2+
11/2+
11/2−
9/2+
11/2+
9/2+
9/2+
11/2−
7/2+
7/2+
7/2+
5/2+
5/2+
5/2+
105
107
109

11

FR 7803602

LYCEN/7757
Juillet 1977

HIGH-SPIN STATES IN $^{104,105}Cd$

J. Genevey-Rivier, J. Tréherne
Institut des Sciences Nucléaires (IN2P3 and USMG)
53, Avenue des Martyrs - 38000 Grenoble (France)

and

J. Danière, R. Béraud, M. Meyer, R. Rougny
Institut de Physique Nucléaire (and IN2P3), Université Lyon-1
43, Bd du 11 Novembre 1918 - 69621 Villeurbanne (France)

ABSTRACT

The $^{104,105}Cd$ nuclei have been investigated in the $^{102}Pd(\alpha, n\gamma)^{104}Cd$, $^{102}Pd(\alpha, n\gamma)^{105}Cd$ and $^{102}Pd(\alpha, 3n\gamma)^{105}Cd$ reactions. The proposed level schemes including states up to 4817.7 keV and 3342.9 keV for ^{104}Cd and ^{105}Cd respectively are based on results obtained from direct and delayed γ-ray spectra, excitation functions, γ-γ coincidences and γ-ray angular distributions. Intense E2 cascades have been observed in ^{104}Cd nucleus. Decoupled bands built on the $\nu h_{11/2}$ and on $\nu g_{7/2}$ are populated in ^{105}Cd.

HIGH-SPIN STATES IN $^{104,\ 105}Cd$.

J. Genevey-Rivier, J. Tréherne.
Institut des Sciences Nucléaires (IN2P3 and USMG)
53, Avenue des Martyrs - 38000 Grenoble (France)

and

J. Danière, R. Béraud, M. Meyer, R. Rougny,
Institut de Physique Nucléaire, (and IN2P3), Université Claude-Bernard
Lyon-I, 43 Bd du 11 Novembre 1918, 69621 Villeurbanne (France).

1 - INTRODUCTION

A considerable amount of experimental work has been done in the Cadmium nuclei, however very scarce information was available on the neutron-deficient ^{104}Cd and ^{105}Cd isotopes. The level structure of ^{105}Cd had been investigated in our group from the $^{105}In \rightarrow Cd$ decay (Rougny et al. 1973, Rivier et al. 1975). Recently in the single neutron pick-up reaction $^{106}Cd(^{3}He, \alpha)^{105}Cd$ performed by Chapman and Dracoulis (1975), eleven states of the final nucleus were identified and corresponding ℓ_n - value assignments extracted.

A striking feature of ^{107}Cd (Hagemann et al. 1974) and ^{109}Cd (Meyer et al. 1975) nuclei is the existence of a decoupled band built on the unique parity $\nu(h\ 11/2)$ state. This led us to search for a similar sequence of high spin states connected by stretched E2 transitions in ^{105}Cd using $Pd(\alpha, xn\gamma)Cd$ reaction.

The study of ^{104}Cd was all the more important as in ^{106}Cd we observed (Danière et al. 1977) additional 6^+ and 8^+ levels probably due to particle excitation. In the case of ^{104}Cd nucleus only the two first excited levels were known from $Mo(^{12}C, xn\gamma)^{104}Cd$ reaction (Hashizume et al.

1969). R. Coussement et al. (1976) observed 3 γ-rays in the (1.7 ± 0.3) min. ^{104}In decay using on-line mass separation techniques. Recently Varley et al. (1977) proposed a more detailed level scheme studying the same decay. The aim of the present work is to identify the high spin states of ^{104}Cd by ^{102}Pd(α, 2nγ)^{104}Cd reaction.

2 - EXPERIMENTAL PROCEDURE AND DATA ANALYSIS

Targets approximately 10 mg/cm^2 of isotopically enriched ^{104}Pd (80%) and ^{102}Pd (78%) were prepared by deposition on thin polyethylene backings. They were bombarded with 1 - 5 nA beams of α particles from the Grenoble variable energy cyclotron.

The γ-ray single spectra measurements were performed with a 40 cm^3 Ge(Li) detector at 45^o to the beam direction. The energy resolution of tbis calibrated spectrometer was 2.2 keV (F.W.H.M) for 1332.5 keV γ-rays of ^{60}Co.

γ-ray spectra were recorded at α bombarding energies ranging from 20 to 53 MeV in order to find the maximum γ-ray yield for ^{104}Cd and ^{105}Cd. These excitation functions led us to fix the energy at 33 MeV for the ^{102}Pd(α, 2n)^{104}Cd reaction. The ^{105}Cd nucleus was studied by two different reactions.: ^{102}Pd(α, n)^{105}Cd at 24 MeV and ^{104}Pd(α, 3n)^{105}Cd at 43 MeV. Typical excitation function curves of the strongest lines in ^{105}Cd are presented in Figure 1 for the ^{104}Pd(α, 3n) ^{105}Cd.

γ-γ coincidences were studied in separate experiments using two Ge(Li) detectors and a fast-slow coincidence circuit with overall time resolution about 10 ns. The coincidences were stored event by event on a magnetic tape connected to a PDP-9 computer. The data matrix was 1024 x 1024 channels and more than 2.10^7 events were stored for each isotope studied. An off-line analysis allowed the reconstruction of coincidence spectra by setting digital gates on the peaks of interest. The spectrum in coincidence with the background due to Compton events has been substracted for each gate.

The γ-γ results were used in connection with the sum rule for the construction of the level scheme.

Additionnal α-γ delayed coincidence measurements were performed in order to search for long-lived levels. For this, γ-ray spectra delayed and not delayed with respect to the high frequency signal of the cyclotron, called respectively "OUT" and "IN" spectra, have been recorded.

The angular distribution experiments were performed with the targets mentioned above. For $^{102}Pd(\alpha, n)^{105}Cd$ reaction, the maximum recoil energy is $\approx$ 1.3 MeV with bombarding α particles of 33 MeV energy. Then the corresponding range of the Cd nuclei is about 0,3 mg/cm^2 in a A = 102 matrix (Northcliffe and Shilling, 1970). Thus at least 98 % of the recoiling nuclei are stopped in our target ; this is corroborated by the fact that the angular distribution spectra do not exhibit any distortion due to Doppler shift.

Beam centering was checked by measuring the angular distribution γ-rays due to the $^{105}Cd \rightarrow Ag$ radioactivity produced in the target (accuracy better than 0.5 %). A third detector located at a fixed position (+60°) was used for beam intensity monitoring. The overall error on the normalization was about 1 % for both nuclei.

The target-to-detector distance was 13.5 cm and the detector was positioned at 5 angles from 90° to 30° backward angles with respect to the beam axis. Two complete cycles were made with 30 minutes counting period at each angle. The angular distributions have been analyzed in a classical way, described earlier by Yamazaki (1967) and Simms et al. (1973) for example, assuming that the nucleus was excited into an approximately aligned state with a Gaussian population of magnetic sub-states centered on m = 0. We have checked the consistency of our measurement by extracting the σ/I values, caracterizing the relative disalignment, from the attenuation of the A_2 and A_4 coefficients.

3. RESULTS FOR ^{104}Cd

In figure 2 is plotted a direct γ-ray spectrum obtained in the $^{102}Pd(\alpha, 2n\gamma)^{104}Cd$ reaction at 33 MeV energy projectile. As an example of γ-γ coincidences, figure 3, shows typical coincidence spectra gated by the 532.9, 840.6 and 890.2 keV γ lines. In these spectra appear the 657.9 ($2^+ \rightarrow 0^+$) and 834.0 keV ($4^+ \rightarrow 2^+$) γ rays unambigously assigned to ^{104}Cd isotope by Varley et al (1977). Table 1 summarizes the properties of γ-rays assigned to this isotope. On figure 4 are plotted the least square fits of angular distribution for the transitions appearing in the strongest cascade of ^{104}Cd. In figure 5 we show one of the direct angular distribution spectra measured at 90^o angle. From α-γ delayed coincidence measurements there is no evidence of a long-lived state in this nucleus ; we now discuss relevant points of our scheme presented in figure 6.

657.9, 1491.9, 2370.0, 3210.7, and 4100.9 keV levels

These levels form the main cascade of the scheme. The angular distributions of the lines involved have been analyzed as mentioned in § 2. The A_2 and A_4 coefficients are consistent both with spin change $\Delta I = 0$ and $\Delta I = -2$. In spite of the absence of "cross-over" transitions the possibility of $\Delta I = 0$, M1-E2 mixed transitions might remain. However the following analysis favours the case $\Delta I = -2$.

Figure 7 shows the consistency check based on the σ/I values analysis. Assuming a Gaussian distribution of the m-substates for the levels of a cascade of stretched E2 transitions, the experimental points are extracted from the A_2 and A_4 coefficients. The solid lines are the theoretical curves normalized on the experimental value of the highest level. When going down in the cascade it is easy to remark, first, a consistent pattern of deorientation and secondly that experimental widths become larger than theoretical ones (side-feeding for example contributes to this effect).

The smooth trend of the relative width shows that our results are compatible with a cascade of stretched E2 transitions.

The 657.7 keV first excited state is unambiguously a 2^+ state. The occurence of a M1-E2 mixed transition with $\delta \simeq 1$ must be considered in the upper members of the cascade. However the B(E2) ratios usually observed [for example $B(E2 ; 2_2 \rightarrow 0)/B(E2 ; 2_1 \rightarrow 0)$] in weakly deformed nuclei are generally of the order of a few percent. If we assume that the 1491.9 keV level is a 2^+ level and analogous B(E2) ratios, the intensity ratio $\frac{I_\gamma(1491.9)}{I_\gamma(657.7)}$ would be of the order of 1. The upper limit for this ratio, deduced from the experimental spectrum is only 10^{-3}. Thus the 1491.9 keV level has definitively spin and parity 4^+. The same deduction applies for upper levels and this leads to propose the following sesequence of spins and parities $0^+ - 2^+ - 4^+ - 6^+ - 8^+ - (10^+)$ for the levels mentioned above.

2114.0 keV level

This level could be the level observed at 2116 keV excitation energy by Varley et al. (1977) in the ^{104}In decay. No spin assignment can be deduced from the angular distribution of the 622.1 keV γ-line because of its complex nature. The $\Delta I = 0, -2$ character of the 321.2 keV γ-line connecting the 6^+ level at 2435.4 keV (as shown in next paragraph) leads to assign I = 6 or 4. The weak feeding of this level indicates that it is not the "Yrast" 6^+ and favours $I = 4^+$.

2435.4 and 2902.0 keV levels

The E2 character of the 775.3 keV leads to assign spin 6^+ for the 2435.4 keV level. The 943 keV peak is of complex nature. The smallest value of the A_2 coefficient of the 943.5 keV line as compared to that expected for a stretched E2 transition is probably due to the presence of the 943.6 line belonging to ^{105}Cd. From the angular distribution results of the strong 532.9 keV transition ($\Delta I = 0, -2$) we assign spin 6 or 8 for the level 2902.0 keV

3903.9, 4038.3 and 4741 keV levels

The $\Delta I = \pm 1$ character of both 1001.0 keV and 827.6 keV transitions gives 5, 7 or 9 as possible spin for the 3903.9 keV level and 7, 9 for the 4038.3 keV level. Taking into account the angular distribution of the 702 keV γ-line, we assign the spin 9, 11 to the 4741 keV level.

4 - RESULTS FOR ^{105}Cd

Table II gives a summary of the data obtained about the γ-rays assigned to ^{105}Cd in the $^{102}Pd(\alpha, n)^{105}Cd$ reaction. In figure 8 a single γ spectrum is presented. The γ-ray intensity ratios reported in table III show that the 126.4 keV - 812.5 keV - 807.8 keV cascade is delayed and partially fed by an isomeric level. This is in agreement with the identification by Heiser et al. (1973) of a 5 μs halflife level at an excitation energy higher than 2517.2 keV. This was confirmed later by Grau et al. (1975). Figure 9 represents two coincidence spectra gated by the 539.3 and 668 keV γ-rays. Let us now discuss in more details the most interesting features of the level scheme shown in figure 10.

g.s. 195.9 and 260.0 keV levels

Spin and parity $5/2^+$ of the g.s. level were assigned by Laulainen and Mc. Dermott (1969) from hyperfine structure studies using the optical double-resonance technique and confirmed in $^{106}Cd(d, t)^{105}Cd$ reaction (Degnan and Rao, 1973) and more recently by Chapman and Dracoulis (1975) in $^{106}Cd(^{3}He, \alpha)^{105}Cd$ reaction. The 195.9 keV level has been already observed by Rougny et al. (1973) in the 5.1 min ^{105}In decay. The angular distribution of the (195 keV $\rightarrow$ g.s.) transition could not be evaluated because of the presence of the 197 γ-line due to ^{19}F activity produced by $^{16}O(\alpha, p)^{19}F$ reaction. Probable spin values are ranging from 1/2 to 9/2.

1162.7, 1702.0, 2488.2, 3343.9 keV levels

Angular distributions of the 832.2, 700.9, 227.8 keV γ-rays are consistent with the spin assignment $I^{\pi} = 5/2^{+}, 9/2^{+}$. The spin change $\Delta I = \pm 1$ deduced unambiguously from the angular distribution of the 330.6 keV γ-line leads to I = 3/2, 7/2, 11/2 for the 1162.7 keV level. This level has been observed at 1162 keV by Chapman and Dracoulis (1975) in the the $^{106}Cd(^{3}He,\alpha)^{105}Cd$ reaction ; they deduced $\ell_n = 4$ or 5 for the transferred neutron eliminating thus the spin value 3/2. Grau et al. (1975) have recently established by linear polarization that this level has spin 11/2 with negative parity.

The angular distributions of the 539.3, 786.2 and 854.7 keV γ-rays are characteristic of stretched E2 transitions. So we assign the spin and parity sequence $11/2^{-}$, $15/2^{-}$, $19/2^{-}$, $23/2^{-}$.

131.1, 799.2, 1685.8, 2587.3 keV levels

For the 131.1 keV level, the result of the angular distribution of the 131 keV γ-ray ($\Delta I = \pm 1$) is in agreement with the reaction data giving $\ell_n = 4$ with $7/2^{+}$ assignment. The angular distributions of the 668.1, 886.6 and 901.5 keV γ-rays are characteristic of stretched E2 transitions : so we assign $11/2^{+}$, $15/2^{+}$, $19/2^{+}$ for the 799.2, 1685.8 and 2587.3 keV levels.

604.1, 770.5, 1578.4, 2390.8 keV levels

From the angular distributions of the 604.1 keV ($\Delta I = \pm 1$), 770.5 keV, 807.8 keV, 812.5 keV ($\Delta I = -2$) γ-rays we propose $7/2^{+}$, $9/2^{+}$, $13/2^{+}$ and $17/2^{+}$ respectively for these states.

832.2, 1728.2 keV levels

The angular distributions of the 832.2, 227.8 and 700.9 keV γ-rays allow to assign unambiguously $I^{\pi} = 9/2^{+}$ for the 832.2 keV level. The large A_2 coefficient of the 896 keV angular distribution favours $\Delta I = -2$ and led us to propose $13/2^{+}$ for the 1728.2 keV level.

5. DISCUSSION

^{104}Cd

We discuss the structure of the ^{104}Cd nucleus (see figure 11) in connection to that of ^{106}Cd and heavier isotopes (Cochavi et al. (1971) for ^{108}Cd and Lumpkin et al. (1974) for ^{110}Cd). Hartree-Fock calculations have been performed using the Skyrme interaction and the potential energy curves versus the deformation exhibits a wide minimum subdivised into two minima for $^{102-106-110}$Cd isotopes (Meyer et al. (1976). This suggests that e.e Cd nuclei are very soft transitional nuclei, with a weak but clear prolate deformation. The heavier isotopes (for instance ^{114}Cd) have been usually interpreted as typical vibrators. However Q_{2^+} values have been measured by Esat et al. (1976) and Maynard et al. (1977) for $^{112-110-108-106}$Cd. The experimental values show a constancy among the isotopes and lie around -0.40 eb, indicating a weak prolate deformation in agreement with the HF calculations, as mentioned above. To explain the existence of cross-over transitions and these large values of Q_{2^+} quadrupole moment, which deviates from the predictions of the purely harmonic vibrational model, many authors have introduced anharmonicities :

- coupling two proton holes to the vibrating Sn core in the so-called particle-core coupling model as Alaga et al. (1967) did
- mixing phonon states up to N=2 as Häusser et al. (1971), Spear et al. (1976) did for ^{112}Cd and $^{112-110-108-106}$Cd respectively, or in a boson expansion technique including terms up to sixth order as derived by Kishimoto and Tamura (1976) for ^{114}Cd.

Such treatments have reproduced the experimental E2 matrix elements data up to the two phonon states.

Another equivalent approach is to consider these e.e nuclei as slightly deformed rotating cores. This rotational aligned coupling scheme has been firstly introduced for odd-A nuclei to explain the results of (HI, xnγ) reactions preferentially populating Yrast states I = j+R and where the particle appears "decoupled to the core" (Stephens et al. (1975) It has been successfully extended to e.e Pd isotopes (A = 106-104-102) by Grau et al. (1976). Even-even Cd isotopes can also be understood as slightly deformed rotors. In this scheme, we observe in ^{104}Cd the ground state band up the 10^+ state, with particular strong feeding up to 6^+ state. Apart from these states, appear between the 6^+ and 8^+ g.s.b. states, additionnal states with possible spin 6, 8 or 3, 4, 5 and in particular a second 6^+ state close to the first one as in ^{106}Cd. These states can be due to $(\pi\, g\, 9/2)^{-2}$, $(\nu h\, 11/2)^2$, $(\nu g\, 7/2)^2$ or $(\nu d\, 5/2\ \nu g\, 7/2)$ configurations. Higher in energy, around 4 MeV excitation energy, combinations of two particles such as $(\nu h\, 11/2\, \nu g\, 7/2)$ with the highest possible spin should give rise to the two first states of a decoupled band 4038.3 (7, 9) and 4741 (7, 9, 11) states. In conclusion ^{104}Cd nucleus appears with a very similar structure to that of ^{106}Cd, characterized by a well fed ground state band with an intruder 6^+ state close to the g.s.b. 6^+ level.

^{105}Cd

In this analysis we put together $^{105-107-109}$Cd isotopes. Their level schemes are presented in figure 12. A band structure has been already observed in ^{107}Cd by Hagemann et al. (1974) and in ^{109}Cd by Meyer et al. (1975). For ^{107}Cd, Dönau and Hageman (1976) have interpreted the three sequences of levels with $\Delta I = 2$ spin difference and connected by stretched E2 cascades, in a core plus particle model taking into account two quasi-neutron coupled to an anharmonic ^{106}Cd core. The results of Häusser et al. (1974) who have measured mean lives and g-factors in ^{107}Cd also support a particle vibration coupling description.

On the other hand, ^{109}Cd has been understood in the framework of particle-plus-rotor model, with a h 11/2 neutron decoupled from the core by Meyer et al. (1975).

For ^{105}Cd nucleus, the most stricking feature of our results is the existence of a $\Delta I = 2$ negative hand which exhibits a spin sequence $(11/2^-, 15/2^-, 19/2^-, (23/2^-))$ and a positive band $(7/2^+, 11/2^+, 15/2^+)$. We must remark that their energy spacings appear quite comparable to that of 0^+ 2^+ 4^+ 6^+ states of the even ^{104}Cd core, in a similar manner as for $^{109-107}$Cd (see figure 13).

Furthermore P. Quentin et al. (1977) have used within the particle plus rotor model, single particle wave function obtained from self-consistent calculations to interpret the properties of odd Cd nuclei. Their preliminary results support our data. So we refer to these $11/2^-$, $15/2^-$, $19/2^-$, $(23/2^-)$ states as rotation aligned states where the angular momentum of the odd-particle (here the 1h 11/2 unique parity neutron orbital) is aligned to that of the core R giving states $I = j + R = j$, $j+2$, $j+4$, etc .. If the character of the $11/2^-$ $\Delta I = 2$ decoupled band remains unchanged, the feeding of this band is less in ^{105}Cd than in $^{107-109}Cd$: when A decreases, the 1h 11/2 neutron orbital lies at higher energy. We can note that the so-called "anti-aligned" states $I = |j-R|$ have not been observed in these $(\alpha, xn\gamma)$ reactions. The $\Delta I = 2$ band built on the 1g 7/2 neutron orbital $(7/2^+, 11/2^+, 15/2^+)$ has been clearly observed in ^{109}Cd and ^{107}Cd, but in ^{105}Cd this decoupled band is much more strongly fed as shown in figure 12. Concerning the band based on the 2d 5/2 orbital, which is rather strongly fed in ^{105}Cd as compared to the heavier isotopes, its character is not clearly defined. This band seems to be perturbed by Coriolis effects because $\Delta I = 1$ and $\Delta I = 2$ transitions both occur. Its decoupled character will probably strengthen when N decreases as in ^{105}Pd, ^{103}Pd ^{101}Pd and it would be worth to follow the evolution of such $5/2^+$ bands in lighter isotopes. In figure 14, are presented the lowest levels of a given spin for the $^{109-107-105}Cd$; one can observe a compression of the whole spectrum when N decreases.

The knowledge of the structure of $^{103-101}Cd$ and some B(E2) values would be a crucial test for the particle plus rotor or particle vibration models.

Acknowledgments

We are very indebted to the Grenoble Cyclotron staff for cooperation during this work. The authors would like to thank Dr. Ph. Quentin for valuable discussions.

Note added in proof

In a recent contribution to the Tokyo Conference, Hashizume et al. (1977) proposed a level scheme for ^{104}Cd obtained via $^{104}Pd(^3He, 3n)$ reaction. They proposed a cascade of 658.3 ($2^+ \rightarrow 0^+$), 834.6 ($4^+ \rightarrow 2^+$), 878.4 ($6^+ \rightarrow 4^+$), 841 keV γ-rays in agreement with our results. The location of the 890 keV γ -line is different in their scheme but our coincidence data (see figure 3) show unambiguously that this γ-ray is in coincidence with the 841 keV line. Instead of our 532.9 keV line, they measured a 538.4 keV γ-ray. This difference is probably due to the strong 539.3 keV γ-ray produced by the $^{104}Pd(^3He, 2n\gamma)^{105}Cd$ reaction.

REFERENCES

- Alaga G., Krmpotic F. and Lopac V., 1967, Phys. Lett., 24 B, 537
- Chapman R. and Dracoulis G.D., 1975, J. Phys. G : Nucl. Phys., 1, 657
- Cochavi S., Mateosian E., Der Kistner O.C., Sunyar A.W., and Thieberger P., 1971, Bull. Amer. Phys. Soc., 16, 642
- Coussement R., De Raedt J., Dumont G., Huyse M., Lhersonneau G., Pacholski S., Pattyn H., Sastry D.L., and Van Klinken J., 1976, Proc. 3rd Int. Conf. on Nuclei far from Stability, CERN 76-13, p. 51
- Danière J., Béraud R., Meyer M., Rougny R., Genevey-Rivier J., and Tréherne J.. 1977, Zeit. Phys. A 280, 363
- Degnan J.H. and Rao C.R., 1973, Phys. Rev., C 7, 2131
- Esat M.T., Kean D.C., Spear R.H. and Baxter A.M., 1976, Report ANU-P/643, The Australian National University, Canberra, Australia
- Grau J.A., Samuelson L.E., Popik S.I., Rickey F.A. and Simms P.C. 1975, Bull. Amer. Phys. Soc., 20, 721
- Grau J.A., Samuelson L.E., Rickey F.A., Simms P.C., and Smith G.J., 1976, Phys. Rev., C 14, 2297
- Hagemann U., Brickmann H.F., Fromm W.D., Heiser C. and Rotter H., 1974, Nucl. phys., A 228, 112
- Hashizume A., Inamura T., Katou T., Tendow Y., Yamazaki T. and Nomura T., 1969, IPCR Cyclotron Progress Report, 3, 57
- Häusser O., Alexander T.K., Mc Donald A.B., and Diamond W.T., 1971, Nucl. Phys., A 175, 593
- Häusser O., Donahue D.J., Hershberger R.L., Latter R., Friess F., Bohn H., Faestermann T., Feilitzsch F. and Loebner K.E.G. 1974, Phys. Lett., 52 B, 329
- Heiser C., Brinckmann H.F., Fromm W.D., Hagemann U., and Rotter H., 1973, Symposium on Nuclear Spectroscopy and Nuclear Theory, Dubna, June 19-23, 81

- Kishimoto T. and Tamura T., 1976, Nucl. Phys., A 270, 317
- Laulainen N. S. and Mc Dermott M. N., 1969, Phys. Rev., 177, 1615
- Lumpkin A. H., Sunyar A. W., Hardy K. A. and Lee Y. K., 1974, Phys. Rev., C 9, 258
- Maynard M., Palmer D. C., Cresswell J. R., Forsyth P. D., Hall I. and Martin D. G. E., 1977, Preprint to be published
- Meyer M., Béraud R., Danière J., Rougny R., Rivier J., Tréherne J., and Barneoud D., 1975, Phys. Rev., C 12, 1858
- Meyer M., Danière J., Letessier J. and Quentin P., 1976, European Conference on Nuclear Physics with Heavy Ions, Caen, September 6-10, 98
- Northcliffe L. C., and Shilling R. F., 1970, Nucl. Data Tables, 7
- Quentin P., Letessier J., Danière J. and Meyer M., to be published
- Rickey F. A., and Simms P. C., 1973, Phys. Rev. Lett., 31, 404
- Rivier J. and Moret R., 1975, Radiochemica Acta, 22, 27
- Rougny R., Meyer-Lévy M., Béraud R., Rivier J. and Moret R., 1973, Phys. Rev., C-8, 2332
- Simms P. C., Anderson R., Rickey F. A., Smith G., Steffen R. M. and Tesmer Jr., 1973, Phys. Rev., C-7, 1631
- Spear R. H., Warner J. P., Baxter A. M., Esat M. T., Fewell M. P., Hinds S., Joye A. M. R. and Kean D. C., 1976, Report ANU-P/657, Australian National University, Canberra, Australia
- Stephens F. S., 1975, Rev. Mod. Phys., 47, 43
- Varley B. J., Cunnane J. C. and Gelletly W., 1977, J. Phys. G : Nucl. Phys., 3, 55
- Yamazaki T., 1967, Nucl. Data Tables, A-3

FIGURE CAPTIONS

Figure 1 — Relative yield versus energy for the strongest γ-rays observed in the reaction $^{104}Pd(\alpha, 3n)^{105}Cd$ at energies ranging from 37 MeV to 48 MeV. Errors on the γ-ray yield due to normalization are about 10% and statistical errors are negligeable

Figure 2 — Direct γ-ray spectrum obtained in the $^{102}Pd(\alpha, 2n\gamma)^{104}Cd$ reaction at 33 MeV energy projectile. Parasitic γ-rays have been identified and are indicated. The other lines reported are the strongest of ^{104}Cd

Figure 3 — Coincident γ-ray spectra measured for ^{104}Cd and gated by :

a) the 532.9
b) 840
c) 890.2 keV γ-rays

Figure 4 — Least-square fits of angular distributions for the strongest γ-rays of ^{104}Cd

Figure 5 — An example of direct angular distribution spectrum measured at 90° angle. All γ-rays for which the angular distribution have been calculated are reported in the figure.

Figure 6 — Level scheme of ^{104}Cd nucleus deduced from our experiments

Figure 7 — Relative width (σ/I_i) of the m-substates distribution for the levels involved in the strongest cascade of ^{104}Cd. The distribution is assumed to be gaussian : the solid line joins the theoretical points normalized on the experimental value obtained for the highest level

TABLE CAPTIONS

Table I : Summary of the γ-ray data for ^{104}Cd from ^{102}Pd(α, 2nγ) reaction. γ lines noted with * are complex and can be placed twice in the scheme. (The energy and intensity of the 559 keV line has been obtained from the coincidence data).

Table II : Summary of the γ-ray data for ^{105}Cd from ^{102}Pd(α, n)^{105}Cd.

Table III : γ-intensity ratios of some transitions delayed ("OUT") or non delayed ("IN") with respect to the high frequency signal of the cyclotron.

Transition (keV)	126.4	812.5	807.8	770.5
γ-Intensity ratio $\left(\frac{OUT}{IN}\right)$	1	0.17	0.035	0.025

Table I

E_γ (keV)		I_γ (E_α = 33 MeV)		Angular distrib. coeff. E_α = 33 MeV A_2	A_4	Assignment E_i →	E_f	ΔI
187.4	(0.2)	10	(5)	+ 0.25 ± 0.14	- 0.18 ± 0.20	3031.1 →	2843.7	0, - 2
307.2	(0.3)	25	(4)	- 0.07 ± 0.06	+ 0.22 ± 0.08	3210.7 →	2902.9	± 1
321.2	(0.2)	53	(7)	+ 0.23 ± 0.04	- 0.12 ± 0.05	2435.4 →	2114.0	0, - 2
414.2	(0.3)	~ 5				4741.4 →	4327.2	
423.3	(0.3)	17	(3)	- 0.16 ± 0.07	- 0.09 ± 0.09	4327.2 →	3903.9	
467.3	(0.3)	10	(4)	+ 0.27 ± 0.22	- 0.10 ± 0.30	2902.9 →	2435.4	
473.7	(0.2)	20	(5)	+ 0.13 ± 0.10	- 0.14 ± 0.13	2843.7 →	2370.0	0, - 2
499.6	(0.2)	54	(10)	- 0.36 ± 0.04	+ 0.04 ± 0.06	3031.1 →	2531.5	± 1
532.9	(0.2)	150	(20)	+ 0.28 ± 0.02	- 0.18 ± 0.03	2902.9 →	2370.0	0, - 2
559	(1)	≃ 15				4463 →	3903.9	
622.1	(0.2)*	{ 60	(25)	+ 0.21 ± 0.02	- 0.06 ± 0.03	3653.2 →	3031.1	
		{ 50	(25)			2114.0 →	1491.9	
634.6	(0.2)	30	(15)			4735.5 →	4100.9	
657.9	(0.2)	1000		+ 0.25 ± 0.01	- 0.12 ± 0.02	657.9 →	0	0, - 2
702.6	(0.2)	42	(7)	+ 0.29 ± 0.04	- 0.13 ± 0.06	4741.4 →	4038.3	0, - 2
716.8	(0.2)	16	(5)			4817.7 →	4100.9	
740.6	(0.3)	15	(5)			4394.4 →	3653.2	
775.3	(0.2)	86	(13)	+ 0.34 ± 0.03	- 0.20 ± 0.05	3210.7 →	2435.4	0, - 2
827.6	(0.2)	45	(8)	- 0.21 ± 0.05	+ 0.11 ± 0.07	4038.3 →	3210.7	± 1
831.0	(0.2)	990	(150)	+ 0.27 ± 0.01	- 0.12 ± 0.02	1491.9 →	657.9	0, - 2
840.6	(0.2)	126	(19)	+ 0.31 ± 0.03	- 0.18 ± 0.05	3210.7 →	2370.0	0, - 2
856.4	(0.3)	10	(5)			3887.5 →	3031.1	
878.1	(0.2)	510	(80)	+ 0.29 ± 0.02	- 0.13 ± 0.03	2370.0 →	1491.9	0, - 2
890.2	(0.2)	113	(16)	+ 0.31 ± 0.03	- 0.14 ± 0.04	4100.9 →	3210.7	0, - 2
927.6	(0.3)	60	(9)	+ 0.09 ± 0.02	- 0.22 ± 0.03	3297.6 →	2370.0	0, - 2
943.5	(0.3)	143	(20)	+ 0.08 ± 0.01	- 0.23 ± 0.02	2435.4 →	1491.9	0, - 2
1001.0	(0.3)	85	(13)	- 0.11 ± 0.02	0 ± 0.03	390[illegible].9 →	2902.9	± 1
1039.6	(0.3)	37	(6)	+ 0.23 ± 0.06	+ 0.05 ± 0.06	2531.5 →	1491.9	0, ± 1
1356.0	(0.3)	15	(5)			3887.5 →	2531.5	

Table II

E_γ (keV)		I_γ (E_α = 24 MeV)		Angul. distrib. coeff. A_2	Angul. distrib. coeff. A_4	Assignment E_i →	E_f	δ_I
126.4	(0.2)	30	(2)	+ 0.02 ± 0.09	- 0.14 ± 0.16	2517.2 →	2390.8	
131.1	(0.2)	1000		- 0.176 ± 0.014	- 0.033 ± 0.016	131.1 →	0	± 1
166.4	(0.2)	36	(3)	- 0.20 ± 0.08	+ 0.11 ± 0.13	770.5 →	604.0	± 1
195.9	(0.2)	260	(14)			195.9 →	0	
227.8	(0.2)	42	(6)	- 0.31 ± 0.09	0 ± 0.14	832.0 →	604.0	± 1
260.0	(0.2)	500	(30)	+ 0.20 ± 0.02	+ 0.030 ± 0.026	260.0 →	0	0, ± 1
330.6	(0.2)	190	(20)	- 0.28 ± 0.03	- 0.01 ± 0.04	1162.7 →	832.0	± 1
392.0	(0.3)	210	(15)	- 0.27 ± 0.03	- 0.02 ± 0.04	1162.7 →	770.5	± 1
415.3	(0.3)	54	(7)					
472.8	(0.3)	35	(6)			604.0 →	131.1	
510.6	(0.3)	200	(100)			770.5 →	260.0	
539.3	(0.2)	330	(30)	+ 0.28 ± 0.03	- 0.13 ± 0.04	1702.0 →	1162.7	0, - 2
570.9	(0.3)	61	(6)	+ 0.17 ± 0.10	- 0.20 ± 0.17	766.8 →	195.9	0, - 2
604.1	(0.2)	300	(20)	- 0.73 ± 0.03	+ 0.10 ± 0.05	604.0 →	0	± 1
639.5	(0.2)	300	(50)	- 0.17 ± 0.03	+ 0.16 ± 0.04	770.5 →	131.1	± 1
668.1	(0.2)	910	(70)	+ 0.30 ± 0.02	- 0.12 ± 0.03	799.2 →	131.1	0, - 2
700.9	(0.2)	61	(6)	- 0.82 ± 0.10	- 0.13 ± 0.15	832.0 →	131.1	± 1
704.9	(0.3)	19	(10)	- 0.73 ± 0.30	+ 0.4 ± 0.4	2390 →	1685.8	± 1
770.5	(0.2)	125	(15)	+ 0.35 ± 0.05	- 0.13 ± 0.09	770.5 →	0	0, - 2
779.2	(0.3)	37	(10)	- 0.85 ± 0.15	+ 0.1 ± 0.2	1578.4 →	799.2	± 1
786.2	(0.2)	130	(20)	+ 0.29 ± 0.05	- 0.14 ± 0.08	2488.2 →	1702.0	0, - 2
807.8	(0.2)	260	(30)	+ 0.30 ± 0.04	- 0.12 ± 0.06	1578.4 →	770.5	0, - 2
812.5	(0.2)	65	(10)	+ 0.14 ± 0.11	- 0.13 ± 0.18	2390.8 →	1578.4	0, - 2
832.2	(0.2)	600	(60)	+ 0.30 ± 0.02	- 0.08 ± 0.04	832.0 →	0	0, - 2
854.7	(0.2)*	42	(5)	- 0.20 ± 0.17	- 0.16 ± 0.27	3342.9 →	2488.2	
						1115 →	260	
886.6	(0.3)	400	(40)	+ 0.29 ± 0.03	- 0.07 ± 0.04	1685.8 →	799.2	
896.0	(0.3)	150	(15)	+ 0.33 ± 0.07	+ 0.05 ± 0.10	1728.2 →	832.0	0, ±1, -2
901.5	(0.3)	70	(10)	+ 0.38 ± 0.10	- 0.29 ± 0.17	2587.3 →	1685.8	0, - 2
915.0	(0.4)	9	(5)			2643.2 →	1728.2	
943.6	(0.4)	20	(4)			1139.5	195.9	
1115.1	(0.4)	17	(5)			1115.1 →	0	
1125.7	(0.4)	11	(10)			1385.5 →	260.0	
1139.8	(0.4)	25	(20)			1139.5 →	0	
1189.3	(0.3)	50	(10)			1385.5 →	195.9	
1385.3	(0.4)	30	(15)			1385.5 →	0	

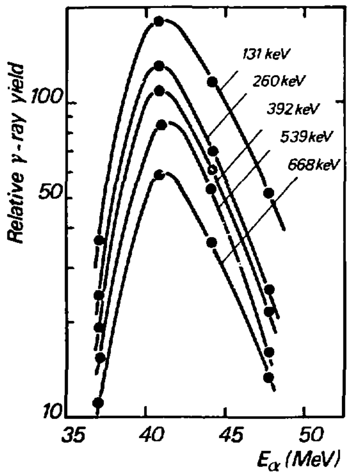

Relative γ-ray yield
100
50
10
35
40
45
50
Eα (MeV)
131 keV
260 keV
392 keV
539 keV
668 keV

FIGURE 1

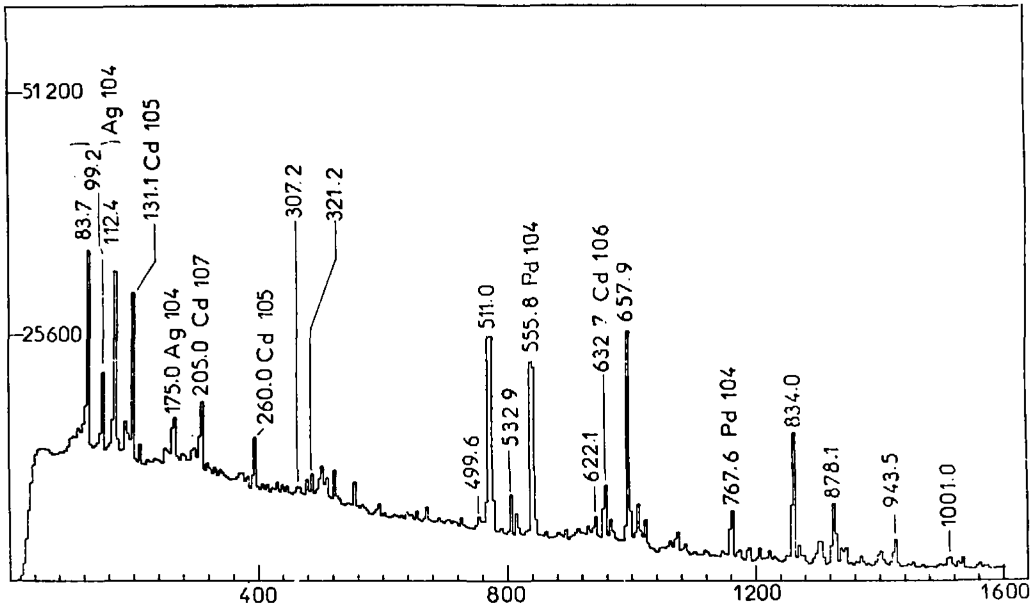
51200
25600
83.7
99.2
Ag 104
112.4
131.1 Cd 105
175.0 Ag 104
205.0 Cd 107
260.0 Cd 105
307.2
321.2
499.6
511.0
532.9
555.8 Pd 104
622.1
632.7 Cd 106
657.9
767.6 Pd 104
834.0
878.1
943.5
1001.0
400
800
1200
1600

FIGURE 2

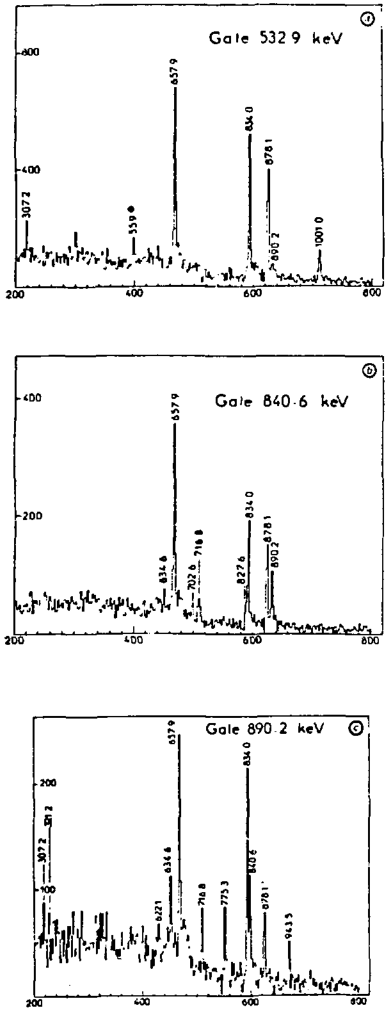

FIGURE 3

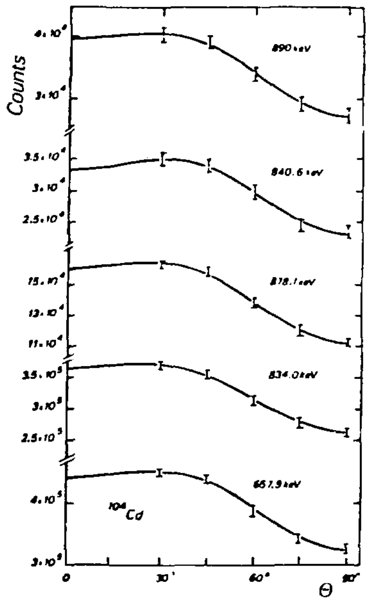

Counts
890 keV
840.6 keV
878.1 keV
834.0 keV
657.9 keV
^{104}Cd
0
30°
60°
90°
Θ

FIGURE 4

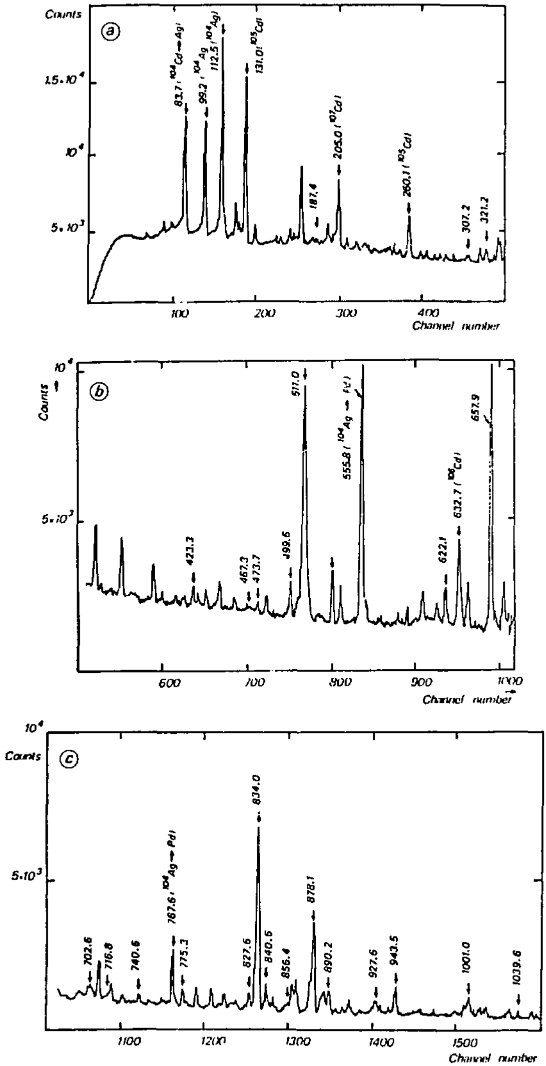

FIGURE 5

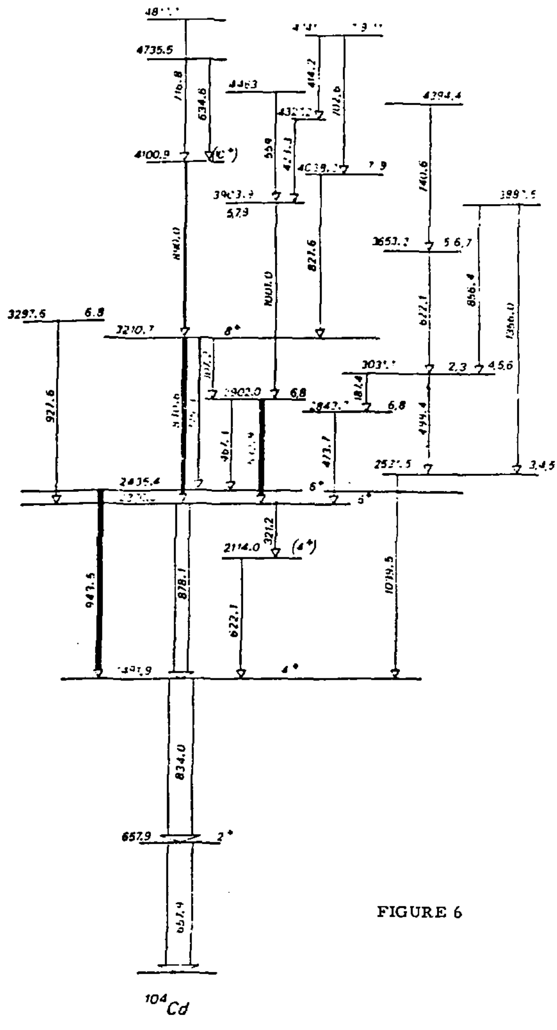
4735.5
4100.9
3297.6
6.8
8+
6+
2114.0
(4+)
4+
657.9
2+
834.0
622.1
321.2
947.5
878.1
1019.5
821.6
1001.0
140.6
856.4
4394.4
3210.7
2902.0
2435.4
^{104}Cd

FIGURE 6

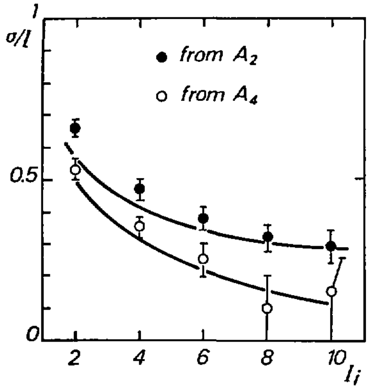

FIGURE 7

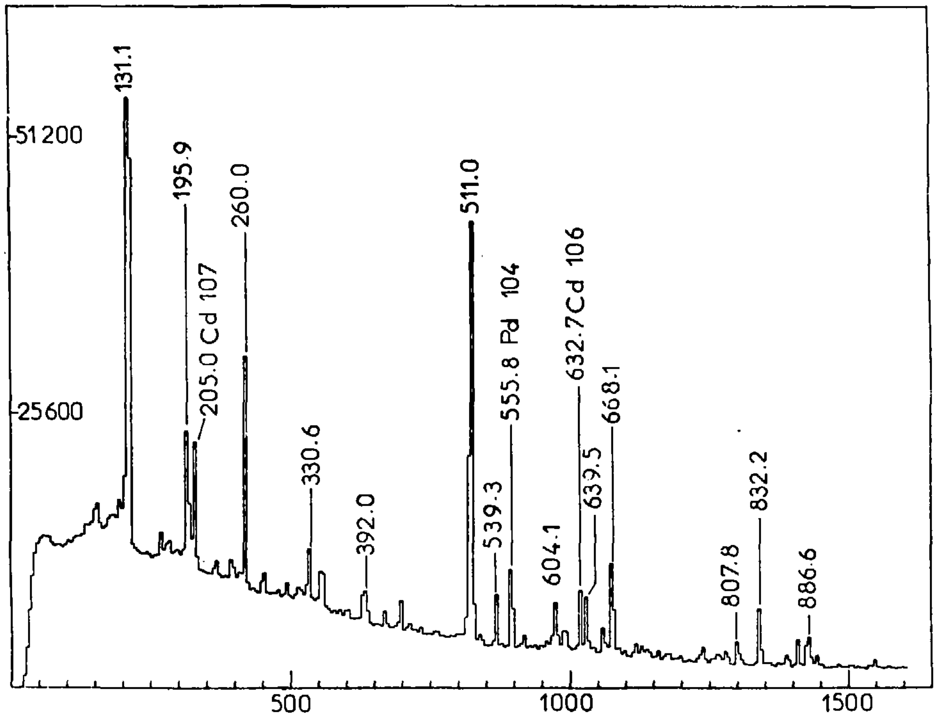
131.1
51200
25600
195.9
205.0 Cd 107
260.0
330.6
392.0
511.0
539.3
555.8 Pd 104
604.1
632.7 Cd 106
639.5
668.1
807.8
832.2
886.6
500
1000
1500

FIGURE 8

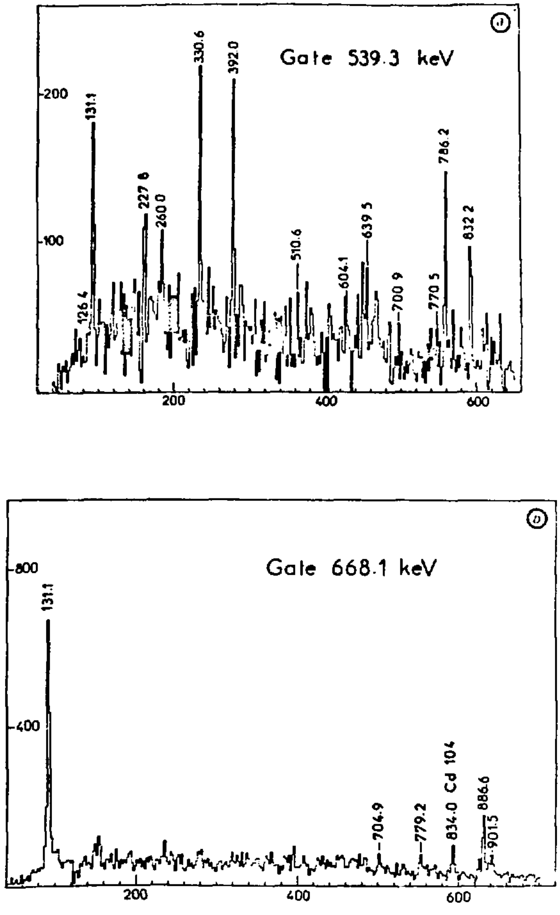

Gate 539.3 keV
200
100
131.1
126.4
227.8
260.0
330.6
392.0
510.6
604.1
639.5
700.9
770.5
786.2
832.2
200
400
600
Gate 668.1 keV
800
400
131.1
704.9
779.2
834.0 Cd 104
886.6
901.5
200
400
600

FIGURE 9

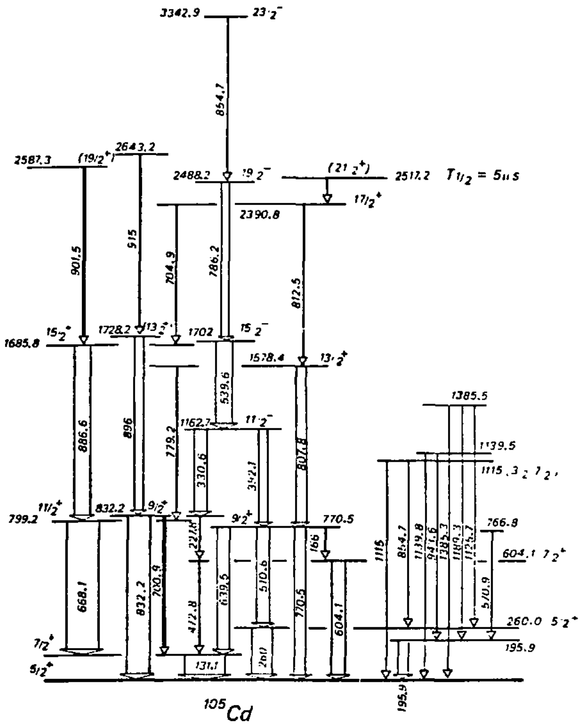
3342.9
23/2⁻
854.7
2587.3
(19/2⁺)
2643.2
2488.2
19/2⁻
(21/2⁺)
2517.2
T1/2 = 5μs
17/2⁺
2390.8
901.5
915
704.9
786.2
812.5
1685.8
15/2⁺
1728.2
13/2⁺
1702
15/2⁻
1578.4
13/2⁺
886.6
896
779.2
539.6
1162.7
11/2⁻
330.6
342.1
807.8
1385.5
1139.5
1115
799.2
11/2⁺
832.2
9/2⁺
9/2⁺
770.5
766.8
668.1
832.2
700.9
227.8
472.8
639.5
510.6
770.5
166
604.1
1115
854.7
1139.8
941.6
1385.3
1189.3
1125.7
510.9
604.1
260.0
195.9
7/2⁺
5/2⁺
131.1
260
195.9
105Cd

FIGURE 10

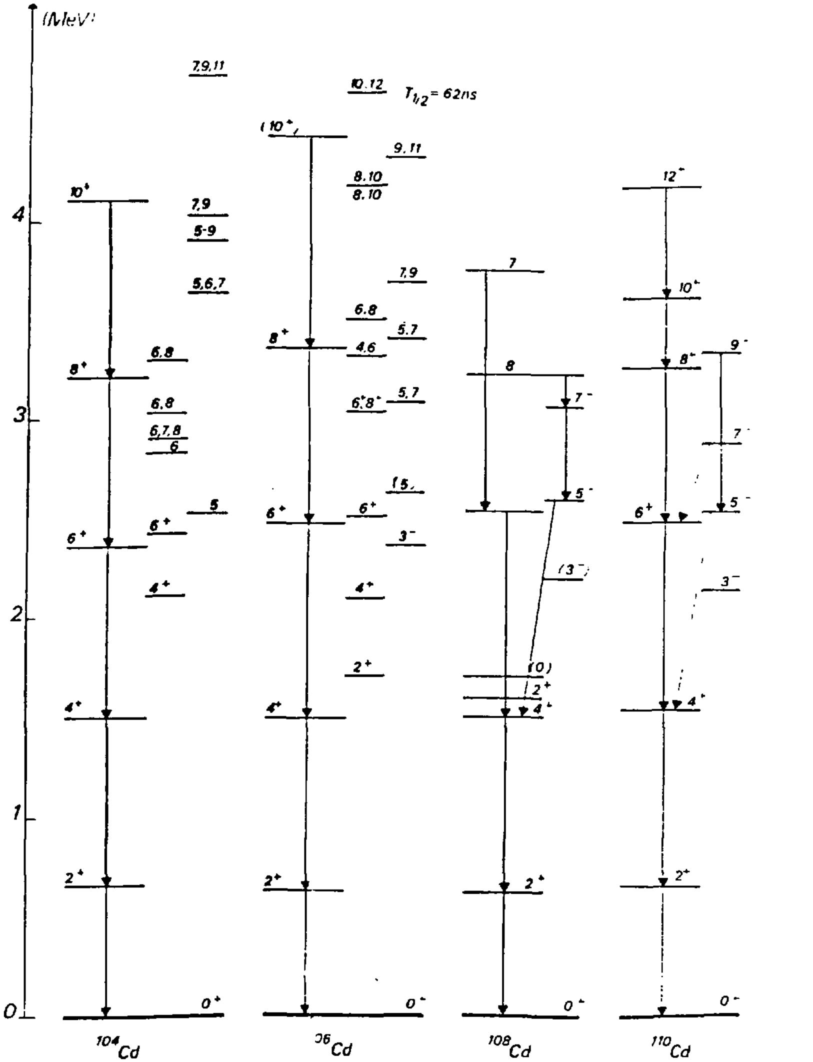

FIGURE 11

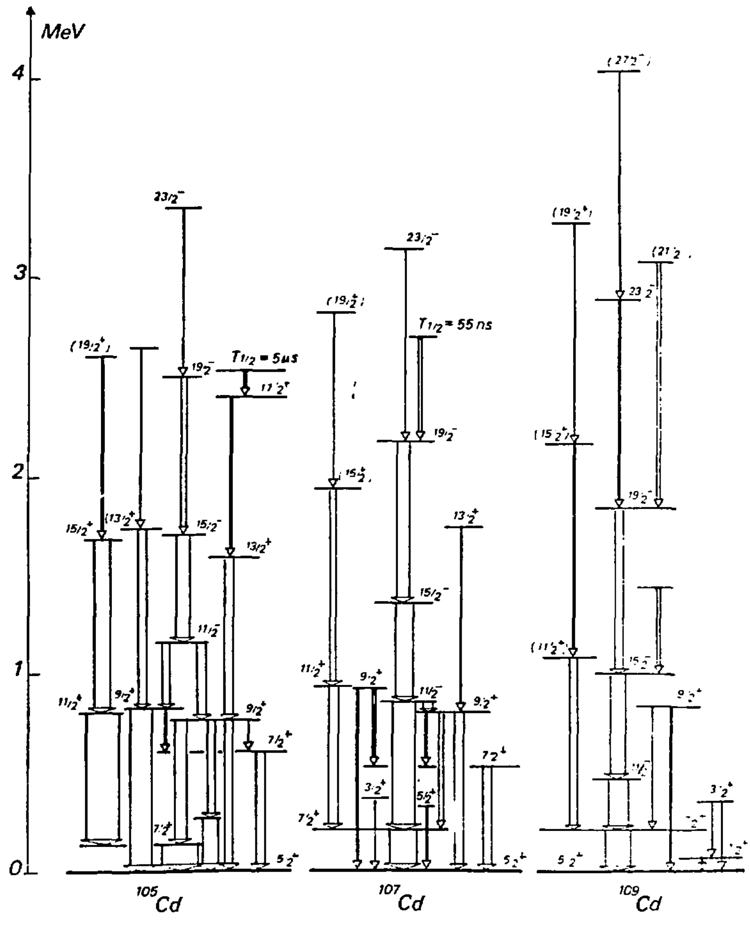

MeV
4
3
2
1
0
105Cd
107Cd
109Cd
T1/2 = 5μs
T1/2 = 55 ns
23/2⁻
(19/2⁺)
15/2⁺
11/2⁺
9/2⁺
7/2⁺
5/2⁺
13/2⁺
15/2⁻
11/2⁻
19/2⁻
(27/2⁻)
(21/2)

FIGURE 12

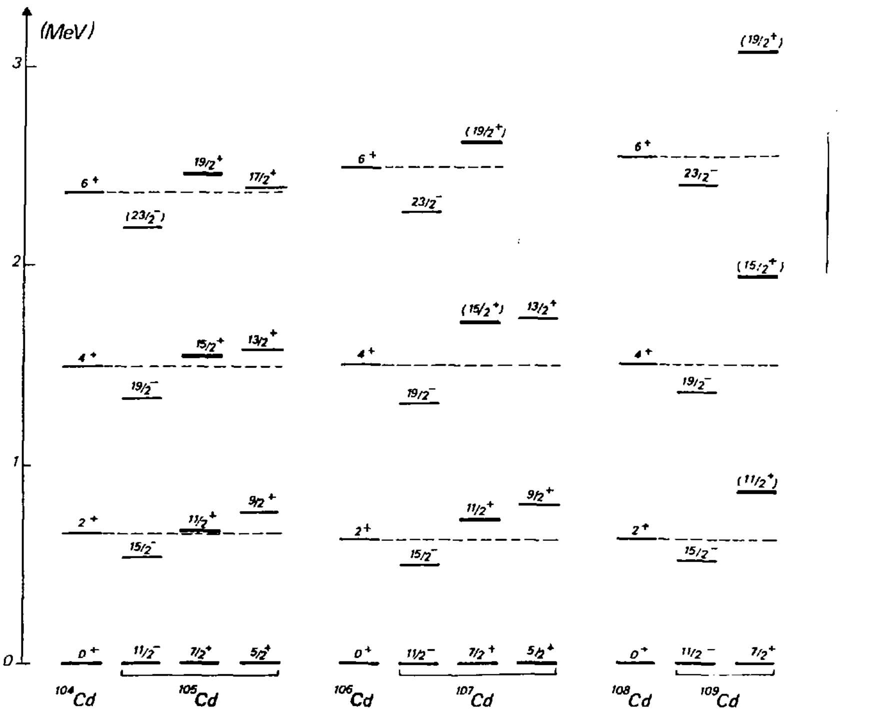
(MeV)
3
2
1
0
0+
2+
4+
6+
11/2−
7/2+
5/2+
15/2−
11/2+
9/2+
19/2−
15/2+
13/2+
(23/2−)
19/2+
17/2+
23/2−
(15/2+)
(19/2+)
(11/2+)
^{104}Cd
^{105}Cd
^{106}Cd
^{107}Cd
^{108}Cd
^{109}Cd

FIGURE 13

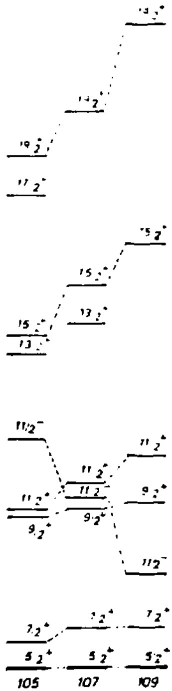

FIGURE 14